POLITECNICO DI TORINO

Master Degree course in Communications and Computer Networks Engineering

Master Degree Thesis

Performance analysis of disaggregated optical networks with adaptive transceiver allocation

Supervisors
Prof. Vittorio CURRI
Dott. Rocco D'INGILLO
Dott. Muhammad Umar MASOOD

Candidate
Gianluigi PERRONE

ACADEMIC YEAR 2024-2025

Abstract

This thesis investigates the performance of fully disaggregated optical transport networks, where network nodes are equipped with a heterogeneous set of commercial transceivers operating in the C-band. In such architectures, transceivers are decoupled from vendor-specific systems, enabling adaptive selection and allocation of transceiver types (100G, 200G, 300G, 400G) based on physical path constraints and traffic demand. This disaggregated model enhances flexibility, spectral efficiency, and scalability, particularly under dynamic network conditions.

To evaluate network behavior, realistic large-scale topologies - USA (USNET), Europe (COST), and Germany (DT) are used within a simulation environment. Performance analysis is conducted using the SNAP (Statistical Network Assessment Process) tool, which applies Monte Carlo-based routing and wavelength assignment (RWA) procedures. It integrates GSNR based Quality of Transmission (QoT) estimations derived from the open-source GNPy engine to simulate transmission impairments across links.

The study demonstrates that adaptive transceiver allocation, guided by GSNR thresholds and link lengths, significantly improves total network throughput while maintaining acceptable blocking probabilities. Additionally, the thesis assesses the impact of Layer 1 encryption on network performance, validating that encryption-enabled transceivers can be integrated into the topology with negligible degradation in traffic handling capability, thus preserving data confidentiality without compromising system efficiency.

Contents

Chapter 1

Introduction

Modern SDN solutions for optical transport networks are typically designed for single-vendor environments, where optical domains operate as independent entities in a fully aggregated deployment model. Although SDN controllers abstract network resources and expose them to higher level through a north-bound interface (NBI), internal mechanisms for resource management, monitoring, and control remain proprietary.

Disaggregated optical networking offers an alternative approach by integrating open and commercially available components, devices, and subsystems to build optical systems. This disaggregation can be partial or complete and is driven by several key factors, including:

- the gap between operators' needs and vendors' ability to provide tailored solutions,
- the increasing commercialization of hardware,
- the varying pace of innovation across different components,
- the potential to accelerate service deployment while reducing operational and capacity costs.

By embracing disaggregation, operators gain greater flexibility in upgrading and migrating components without being tied to a single vendor. However, this model requires careful trade-offs between performance, vendor support, and cost efficiency. Open and standardized interfaces are crucial in this context, as they enable a more unified and model-driven approach to network development. To become more efficient and manageable, improvements in configuration management are essential [1].

The continuous increase in internet data traffic is primarily driven by the growing number of connected devices and the development of new technologies, such as cloud computing, HD streaming, other high-bandwidth applications, and the rapid rise of 5G and 6G technologies.

The impact of transmission layer technology is typically evaluated for point-to-point connections operating at maximum capacity, which is regarded as the optimal scenario. However, due to constraints such as wavelength and spectrum competition, it is not feasible to fully utilize the entire spectrum in fiber networks.

As a result, efforts are increasingly focused on optimizing the utilization of existing infrastructures, primarily to mitigate the rising costs associated with traffic growth. This is being achieved through the adoption of innovative and efficient techniques.

One of the most effective approaches currently being pursued is Wavelength Division Multiplexing (WDM) [2], which enables full utilization of the frequency spectrum, thus optimizing fiber utilization.

This thesis explores the optical transport networks, with a particular focus on network components ranging in the C-band in disaggregated optical networks. The analysis is performed using a simulation tool specialized in the evaluation of the performance of a network.

Finally, a further analysis is performed considering the effect of the Layer 1 encryption on the network traffic allocation.

1.1 Thesis overview

This thesis analyzes the disaggregated optical network transmission systems, with a particular focus on the capabilities of C-band transceivers in an adaptive transceiver allocation approach.

Chapter 2 provides an in-depth examination of the optical network architecture, with a focus on disaggregated networks and the exploration of physical layer propagation modeling. This chapter offers a comprehensive foundation of knowledge essential for assessing network design and performance.

Chapter 3 provides a comprehensive overview of the simulation tools that have been utilized in this study and analyzes the result obtained using three different network topologies.

Chapter 4 focuses on the Layer-1 encryption characteristics and investigates the impact of the encryption on the network performance.

Chapter 2

Optical Networks

2.1 Optical network structure

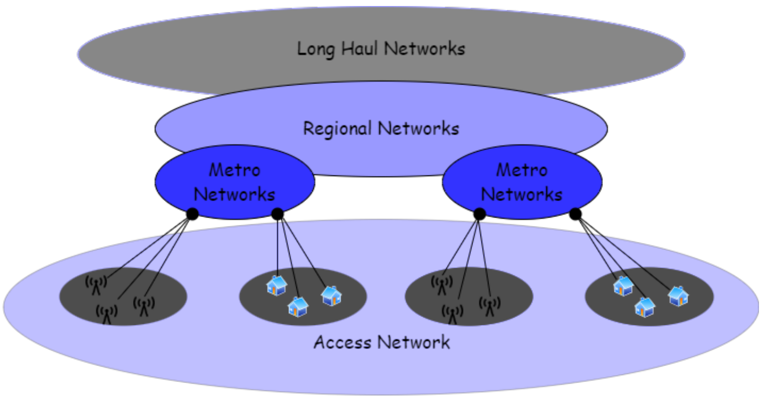

Figure 2.1: Optical Network structure

Figure 2.1 provides a visual representation of the hierarchical structure of communication networks. At the top of the hierarchy are the long-haul (backbone) optical networks, which cover distances ranging from hundreds to thousands of kilometers [3]. These networks are designed to support high-capacity optical communication over vast distances, often connecting different countries or even continents.

Long-haul networks utilize Dense Wavelength Division Multiplexing (DWDM) technology, enabling multiple data streams to be transmitted simultaneously over a single optical fiber. Each stream is assigned a specific wavelength within the DWDM system, allowing these networks to achieve exceptional capacity. In fact, some long-haul networks can transmit terabits of data per second over a single fiber.

The second level consists of regional optical networks, that form the backbone of modern communication infrastructure within specific geographic areas. These networks facilitate seamless data transfer between metropolitan hubs and rural regions, acting as critical intermediaries that bridge the expansive long-haul networks with densely connected metropolitan networks in urban areas.

To ensure high performance and reliability, regional networks use advanced optical transport technologies, such as optical amplifiers and wavelength-selective switches. These technologies optimize data transmission, enabling regional networks to efficiently manage the flow of data while maintaining exceptional capacity and operational efficiency. Optical amplifiers enhance the strength of the signal, allowing data to be transmitted over longer distances without significant degradation. Meanwhile, wavelength selective switches (WSS) ensure precise routing of data streams to their intended destinations, optimizing the efficiency and reliability of data transfer within the network. This level plays a vital role in enabling seamless communication within various regions.

The third tier comprises Metro Optical Networks, also known as Metropolitan Area Networks (MANs), which are essential for enabling communication across densely populated urban areas. Positioned in cities, these networks serve as critical intermediaries, connecting regional networks to access networks, and thus form a key component of the overall communication infrastructure.

Reconfigurable Optical Add-Drop Multiplexers (ROADMs) are employed in metro networks to enable flexible and dynamic traffic routing. This adaptability allows for the efficient use of network resources, ensuring both high reliability and performance in the ever-changing landscape of metropolitan areas. Designed to address the increasing demand for high-bandwidth services, metro optical networks prioritize low latency, high scalability, and efficient traffic grooming. Low latency is particularly critical for real-time applications where minimal delays are essential for seamless interaction. Due to the high scalability these networks it is possible to effectively accommodate the growing volume of data traffic, while efficient traffic grooming optimizes resource utilization, enhancing both performance and cost-effectiveness.

As the backbone of urban communication infrastructure, metro optical networks provide uninterrupted connectivity and are tailored to meet the diverse needs of modern metropolitan communities [4].

In the context of optical network architecture, access optical networks represent the final stage in the process of providing high-speed internet access, video streaming services and other communication solutions directly to end user. These networks are of particular importance as they act as the gateway point for end-users, enterprises and residential areas. In order to cater to customers' different demands and provide efficient and reliable access, access networks use passive optical networks (PONs) [5] and Ethernet-based solutions [6].

2.2 Software Defined Networking

The objective of Software-Defined Networking (SDN) [7] is to reduce the digital gap and provide universal access to the benefits of contemporary communication technologies. SDN has been identified as a solution to the aforementioned challenges, through the introduction of programmable network architectures that enable dynamic and centralized control over network resources. SDN introduces a logically centralized control plane separated from the data plane; in this way it is possible to centrally manage and configure network behavior using software-based controllers, which can be executed on general-purpose hardware.

In practice, SDN creates the basis for a network infrastructure that is not only scalable and programmable but also flexible enough to adapt to the ever-changing demands faced by network operators. The implementation of SDN through open standards has been shown to facilitate the processes of network design and operation. This is due to the fact that SDN controllers provide instructions, as against those provided by multiple vendor-specific devices and protocols [8]. SDN architecture, shown in Fig.2.2, consists of data plane, control plane, and management plane [9].

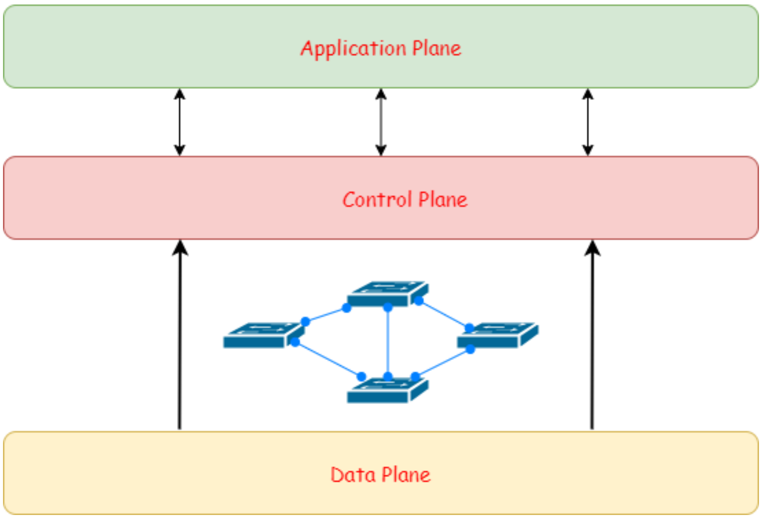

Figure 2.2: SDN architecture

2.2.1 Data plane

The data plane consists of two sub-layers: the infrastructure layer and the southbound interface. The infrastructure layer includes physical switches, which, due to centralized control, function solely as data forwarding components. These switches operate based on the data forwarding mechanisms defined by the controller. These mechanisms are essentially sequences of flow tables containing rules that are compared against incoming packets. The purpose of this comparison is to determine the appropriate actions to execute when a match is identified.

2.2.2 Control plane

The control plane functions as the brain of SDN. A key advantage of centralizing logical control, rather than relying on physical control, is the ability to deploy backup controllers, thereby overcoming the risk of a single point of failure [10]. In control plane, three sub-layers are distinguished: network hypervisor, network operating system (NOS), and northbound interface.

Network hypervisor permits to enable efficient resource utilization by transforming physical network infrastructure into virtualized components. The hypervisor acts as an intermediate layer between the controller and the virtual SDN networks and can control the traffic exchanged between them. [11]

Network operating system (NOS) is the core of the control plane, it provides the traffic management and control. It offers a mechanism to manage hardware and network components via software. NOS significantly improves network agility and facilitates the seamless integration of a wide range of network services and applications.

The Northbound interface serves as the interface between the SDN controller and upper-layer applications. It allows applications to communicate their requirements to the network, which then allocates the necessary resources. This enables dynamic network configuration and efficient resource utilization. As a critical component of the SDN stack, the Northbound API acts as an abstract programmable interface for management and application systems. It provides essential network functions to users, translates application requests into vendor-specific configurations, and ensures seamless communication with network nodes. Its primary goal is to extract abstracted data models and functionalities within the controller, supporting a wide range of applications with diverse requirements. [11]

2.2.3 Management plane

The management plane (or application layer) sits above the control plane and enables the execution of various applications to perform flexible operations essential for maintaining an efficient network. Applications running in the management plane communicate with the controller via northbound API, which then executes the corresponding actions in the data plane.

2.3 Disaggregated optical networks

Disaggregated optical networks (DON) within the SDN framework are transforming the management and control of optical communication infrastructure. To promote interoperability among vendors and reduce deployment costs, multi-source agreements (MSAs) have been established to define standardized data models and interfaces for optical networking equipment. By embracing the concept of disaggregation, these networks enable the independent management of diverse network elements from multiple vendors, including amplifiers, Reconfigurable optical add-drop multiplexers (ROADMs) [12], and transceivers. Disaggregation can occur at two levels, Fig.2.3: complete disaggregation, where each network element is managed individually, or partial disaggregation, where entire Optical Line Systems (OLSs) are managed as independent units.

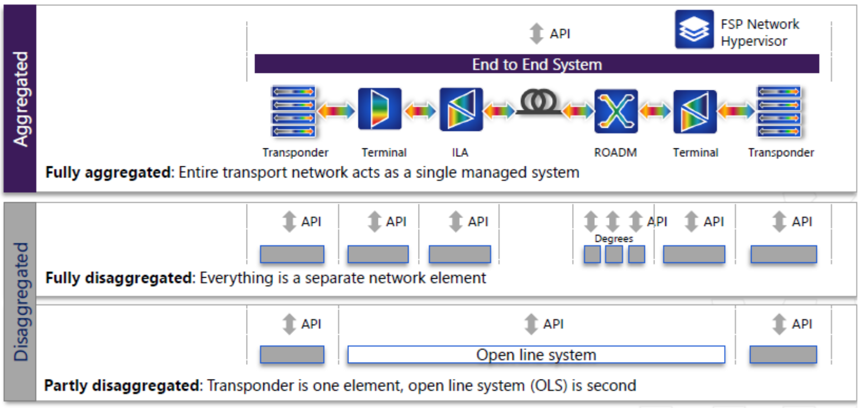

Figure 2.3: SDN architecture

This approach enhances flexibility and interoperability within the network by enabling seamless integration and management of equipment from multiple vendors, using open, non-proprietary protocols. Interoperability ensures that the central optical network control can efficiently oversee and manage both hardware devices and the entire network. This encompasses tasks such as configuration, performance monitoring, and fault management leads to more efficient resource utilization and simplified network management. In this thesis, it is assumed a fully-disaggregated optical network, where all the configurations of the OLS are set and maintained by a unified control plane. This method provides a multitude of benefits, such as increased adaptability, expandability, and impartiality towards vendors. Organizations may enhance their optical communication infrastructure and easily react to changing network requirements by adopting the notion of disaggregated optical networks within the context of SDN.

2.4 Characterization of the physical layer

An Optical Line System (OLS) is illustrated in Fig. 2.4:

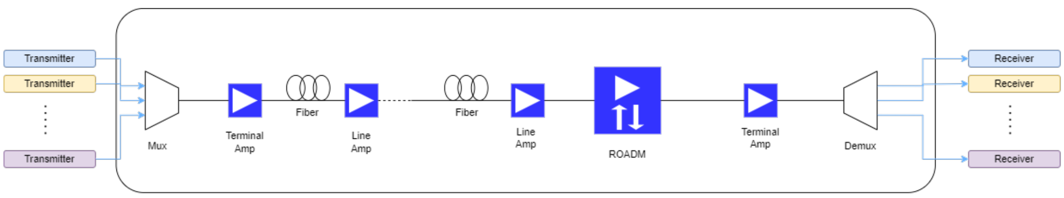

Figure 2.4: Optical line system

Initially, N transmitters convert electrical signals into optical signals, each at a unique frequency for multiplexing, enabling transmission via optical fibers. The multiplexed signals then pass through a ROADM node for fiber interconnection. Along the transmission path, optical amplifiers, such as EDFA or TDFA, are utilized to counteract signal attenuation, while fiber segments ensure signal transmission over specific distances. In the final phase, the signals are routed through additional fibers connected to the main ROADM node or demultiplexed and sent to N receivers, where the conversion into digital signals is performed.

2.4.1 Coherent transceiver

In modern optical communication systems, coherent transmitters and receivers have been introduced enabling the use of multilevel modulation formats and enhancing the capacity and the efficiency of optical networks. These devices boost data throughput by encoding information into multiple dimensions of the light wave, achieved through the modulation of in-phase (I) and quadrature (Q) components across the two orthogonal polarizations (X and Y) of an optical carrier.

The structure of a coherent optical transmitter, illustrated in Fig. 2.5, comprises a laser source, polarization beam splitters (PBSs), and Mach-Zehnder modulators (MZMs). The process begins with the generation of a coherent laser beam, serving as the optical carrier for the transmitted information. This beam is divided into two orthogonal polarizations, vertical and horizontal, by the PBSs, facilitating the dual-polarization technique. This approach allows separate control of the in-phase (I) and quadrature (Q) components for each polarization. The polarized beams are then modulated using MZMs to encode the I/Q components onto the light wave. This is achieved by precisely manipulating the optical phase and amplitude of the carrier wave to represent the encoded digital data. After modulation, the polarized beams are recombined using another set of PBSs, merging the individually modulated signals into a single composite optical signal.

The laser frequency is finely tuned to center the transmission at a specific frequency, optimizing it for WDM techniques [13]. This method enables the simultaneous transmission of multiple channels through a single optical fiber, significantly enhancing the system's capacity.

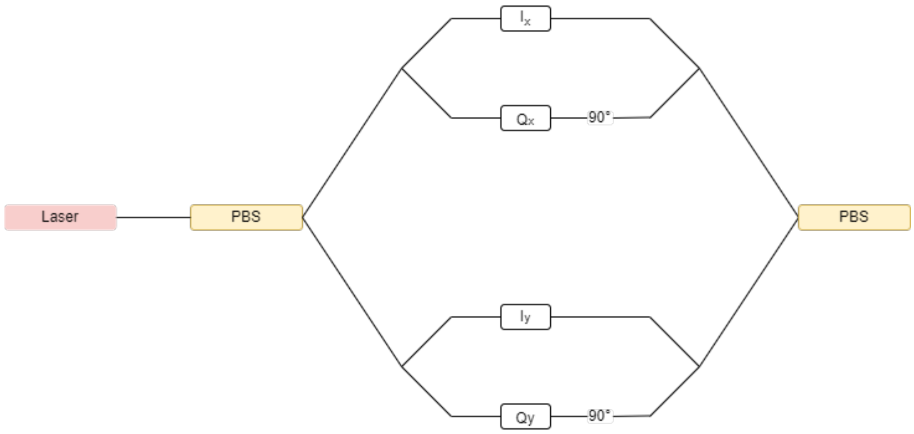

Figure 2.5: Structure of a coherent optical transmitter

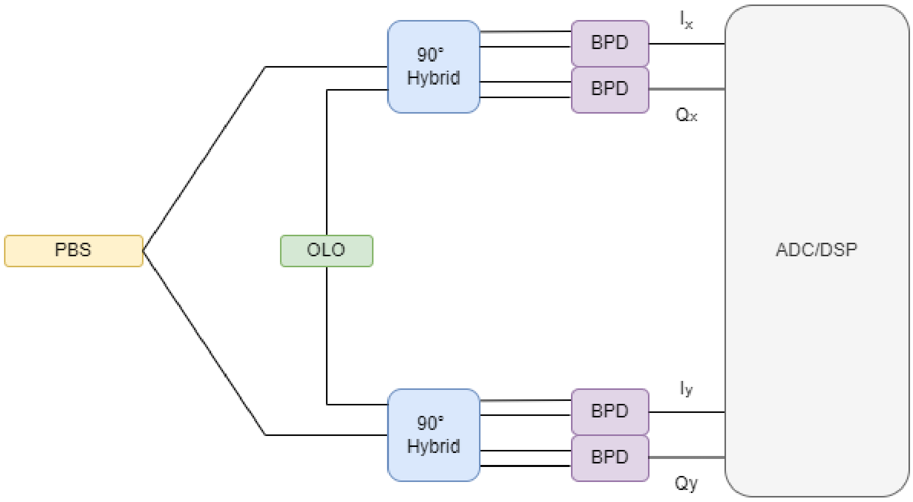

Figure 2.6: Structure of a coherent optical receiver

The coherent receiver, depicted in Fig. 2.6, plays a critical role in accurately demodulating the incoming optical signal within the transmission system. The process begins with the incoming signal being passed through a polarization beam splitter (PBS), which separates it into its individual polarization components [14]. Each polarization is then combined with a reference signal from an optical local oscillator (OLO) using a 90-degree optical hybrid.

The optical hybrid, a passive device made up of 3 dB couplers and a 90-degree phase rotator, facilitates the combination of the incoming optical signal with the local oscillator reference. This combination enables the extraction of the in-phase (I) and quadrature (Q) components for each polarization. The resulting optical signals are sent to balanced photo-detectors (BPDs), which convert them into electrical signals representing the I/Q components.

These electrical signals are further processed by analog-to-digital converters (ADCs), which digitize them for analysis by digital signal processing (DSP) units. The DSP stages are meticulously designed to recover the phase and amplitude information from the received signals while compensating for transmission impairments such as chromatic dispersion and polarization-mode dispersion [15]. This sophisticated processing ensures the accurate reconstruction of the transmitted data, underscoring the reliability and efficiency of coherent transmission systems in modern optical communications.

2.4.2 Analysis of propagation impairments

Attenuation

Attenuation, defined as the reduction in signal intensity as it propagates through an optical fiber, is a crucial factor in the design of optical transmission systems. This phenomenon arises from various factors, including Rayleigh scattering, absorption in the ultraviolet and infrared ranges, peaks in hydroxyl ion absorption, and absorption caused by phosphorous in the fiber core. These elements collectively determine the fiber's attenuation properties, quantified by the attenuation coefficient (α), typically expressed in dB/km [16, 17].

In wide-frequency-range applications utilizing WDM technology, understanding the attenuation dynamics of the fiber becomes vital. The frequency-dependent attenuation coefficient, represented as $\alpha(f)$, highlights the importance of modeling attenuation as a frequency function to accurately assess its impact on signal transmission. Optical power exponentially decays as a function of fiber length and the attenuation coefficient's frequency dependence, providing a foundational tool for evaluating the efficiency of optical transmission systems in mitigating fiber attenuation.

A comprehensive understanding of fiber attenuation is essential for the precise prediction of system performance and plays a critical role in the design and optimization of optical networks.

Polarization-Mode Dispersion

Polarization-Mode Dispersion (PMD) is a critical factor that impacts signal quality in optical transmission systems. It primarily arises due to the inherent birefringence of optical fibers, which causes a temporal delay difference between two orthogonally polarized light modes as they propagate through the fiber. This phenomenon occurs even in single-mode fibers [18]. The primary cause of PMD are small deviations from perfect cylindrical symmetry in the fiber, typically due to random variations in the geometric structure of the core along its length. These irregularities disrupt the uniform propagation conditions, leading to a differentiation between the two polarization modes and causing their interaction and mixing.

The impact of PMD is particularly pronounced in high-speed, long-haul optical networks, where even minor variations in the arrival times of polarization states can lead to signal distortion and an increase in the bit-error rate (BER). However, in coherent optical communication systems, the challenge posed by PMD is significantly mitigated through the use of advanced digital signal processing (DSP) techniques at the receiver. By incorporating adaptive equalization methods, these DSP techniques provide a robust approach to counteracting PMD. Such methods allow for the realignment of orthogonally polarized light components into a coherent signal by dynamically correcting the temporal dispersion effects caused by PMD. The success of DSP in mitigating PMD hinges on its ability to adjust in real-time to the changing dispersion characteristics of the fiber, which can be affected by environmental conditions and physical factors.

Therefore, the operational threshold for PMD tolerance in optical transceivers is a critical design parameter, determined by manufacturers through comprehensive system evaluations and performance criteria. These PMD specifications are essential for the system's design, ensuring that the transmission quality stays within acceptable limits under typical operating conditions. As a result, adhering closely to these requirements during system deployment is vital. Doing so guarantees the establishment of reliable communication links capable of supporting the specified data rates and transmission distances without compromising performance.

Non-linear Kerr effect

The Kerr effect is a fundamental nonlinear optical phenomenon in which the refractive index of a material changes proportionally to the intensity of light passing through it [19]. In WDM optical communication systems, the Kerr effect significantly impacts the Quality of Transmission (QoT) of the signals. A key parameter for characterizing this effect in optical fibers is the nonlinear coefficient, denoted as γ, typically expressed in units of $\mathrm{W}^{-1} \cdot \mathrm{km}^{-1}$. This coefficient quantifies the strength of the Kerr effect: higher values of γ indicate a stronger influence on signal propagation through the fiber.

In WDM systems, the Kerr effect manifests through the following nonlinear phenomena, which contribute to signal distortions:

- Self-Phase Modulation (SPM): SPM causes pulse broadening due to a self-induced phase shift proportional to the pulse's instantaneous power. This modifies the pulse's phase spectrum, leading to temporal spreading.
- Cross-Phase Modulation (XPM): XPM occurs when the intensity of one co-propagating signal induces a phase shift in another, resulting in inter-channel interactions and signal distortion.
- Four-Wave Mixing (FWM): FWM arises from interactions between two or more different wavelengths, generating new frequencies. This leads to unwanted spectral components, causing crosstalk and degrading signal quality in WDM systems.

Chromatic dispersion

Chromatic dispersion (CD) is a key factor that influences the performance of optical transmission systems, characterized by the temporal spread of optical pulses as they travel through a fiber [17]. CD occurs because the refractive index of the fiber varies with wavelength, causing different components of a pulse at varying wavelengths to travel at slightly different speeds. As a result, the pulse broadens, which can limit the system's maximum data transmission rates and decrease the effective transmission distance [19].

Optical fiber manufacturers usually include the zero-dispersion slope S_0 in their datasheets, providing vital data for designing systems that reduce the impact of dispersion [20].

In high-performance coherent optical systems, DSP techniques at the receiver are employed to effectively compensate for chromatic dispersion and its higher-order effects. This compensation is essential for maintaining signal quality over long distances and high data rates, ensuring the system stays within the maximum chromatic dispersion limits specified by the transceiver design.

Stimulated Raman Scattering

Stimulated Raman Scattering (SRS) is a nonlinear optical phenomenon where an incident photon at frequency ω_p interacts with molecular vibrations of a medium, resulting in the generation of a new photon at a lower frequency ω_s, referred to as the Stokes frequency. This process significantly influences light propagation in optical fibers, particularly in WDM systems. The frequency shift ($\Delta\omega$) between the pump (ω_p) and Stokes (ω_s) waves corresponds to the vibrational frequency of the medium's molecules and is expressed as $\Delta\omega = \omega_p - \omega_s$.

The Raman gain spectrum, $G_R(\Delta\omega)$, determines the efficiency of the frequency shift, typically spanning approximately 40 THz below the pump wave frequency in optical fibers like SSMF. The maximum gain is observed at a frequency shift $\Delta\omega_{\max}$, around 13.2 THz for silica fibers, where the Stokes wave undergoes maximum amplification. The Raman gain spectrum for an SSMF is illustrated in Fig. 2.7.

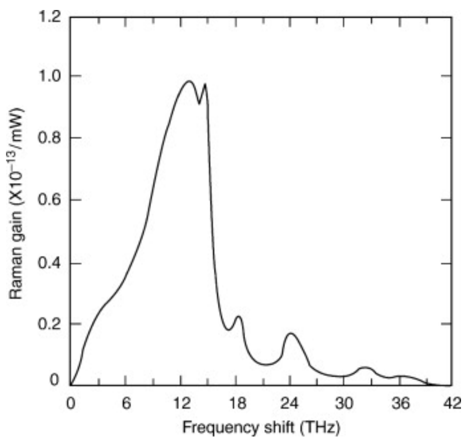

Figure 2.7: Normalized Raman efficiency vs the frequency shift for SSMF [21].

The efficiency of power transfer to the Stokes wave, in high-power scenarios, increases substantially, characterized by the exponential growth of Stokes power relative to fiber length and input pump power. In extreme cases, nearly all pump power can be converted into Stokes wave power, profoundly affecting signal propagation in the fiber. SRS effects can create power imbalances between wavelength channels, where shorter-wavelength (higher-frequency) channels lose power to longer-wavelength (lower-frequency) channels within the Raman gain spectrum . To address this, precise channel power management is required, ensuring that the channel power, P_{ch}, stays below a critical threshold, P_{critical}, beyond which SRS-induced losses become substantial.

Amplified spontaneous emission noise

Amplified spontaneous emission (ASE) noise is a significant source of non-linear interference in optical communication systems, arising primarily from the intrinsic properties of optical amplifiers. For EDFA, ASE noise is generated by spontaneous emission within the gain medium as the optical signal is amplified. This noise is typically modeled as additive White Gaussian Noise (AWGN) with a bilateral power spectral density (PSD), accounting for both polarization modes due to the amplifier's operation [22]. The G_{ASE} equation can be written in function of the noise figure (NF), F, which indicates the amplifier's noise performance:

$$G_{\text{ASE}} = hf_0F(G-1) \tag{2.1}$$

This equation highlights the relationship between the noise figure, gain, and carrier frequency in determining the ASE noise output of the amplifier.

Optical Amplifiers

Optical Amplifiers (OAs) are critical components in modern optical transmission systems, enabling the direct amplification of light signals in the optical domain without requiring conversion to electrical signals. These amplifiers are strategically integrated into the Optical Line System (OLS) to enhance performance and mitigate signal degradation over long-distance transmissions. Their deployment can be categorized based on their position and function within the network:

- Booster Amplifiers: Placed immediately after the ROADM, booster amplifiers compensate for signal losses incurred during ROADM processing. By increasing the signal power at the start of transmission, they help ensure that the optical signal maintains adequate strength as it propagates through the fiber.

- Inline Amplifiers (ILAs): Deployed at regular intervals along the fiber link, ILAs counteract the gradual attenuation of optical signals during transmission. These amplifiers restore signal power, thereby extending the reach of the system while preserving signal integrity.

- Pre-Amplifiers: Positioned just before the optical signal reaches the receivers, pre-amplifiers are essential for improving the Signal-to-Noise Ratio (SNR) and the detection sensitivity of the receiver. This enhancement is especially critical after the signal has traversed long distances, ensuring reliable and accurate signal detection.

To address power loss and signal degradation, three primary types of optical amplifiers are commonly used:

- Semiconductor Optical Amplifiers (SOAs): SOAs are active devices fabricated from semiconductor materials, utilizing current injection to amplify optical signals. They leverage the gain medium's properties to boost signal strength [23]. SOAs are versatile and widely applicable in various optical networking tasks, including switching and signal regeneration.

- Doped Fiber Amplifiers (DFAs): DFAs, the most commonly used amplifiers in long-haul optical systems, employ optical fibers doped with rare-earth elements like Erbium or Thulium as the gain medium [24]. Amplification is achieved through stimulated emission: an external pump laser excites the dopant ions, which release their stored energy as additional photons coherent with the signal, thus amplifying it.

- Raman Amplifiers: Raman amplifiers utilize the Stimulated Raman Scattering (SRS) effect, wherein power from a high-intensity pump laser is transferred to the signal light within the transmission fiber [25]. This technique enables effective in-line amplification by leveraging the fiber's inherent nonlinear properties, thereby extending transmission distances and improving overall system performance.

A crucial consideration in the design and modeling of these optical amplifiers is the management of Amplified Spontaneous Emission (ASE) noise. ASE noise, arising from spontaneous emission in the amplifier's gain medium, adds to the noise background and can degrade the system's SNR. The ASE noise power for a channel centered at frequency f is a function of the amplifier gain $G(f)$ and the noise figure $NF(f)$.

Accurate modeling of ASE noise is essential for evaluating SNR and, consequently, the overall performance of optical transmission systems. By understanding and optimizing the behavior of OAs, networks can be designed to maximize signal integrity and capacity over extended transmission distances.

Quality of transmission

The accurate modeling of signal propagation within optical fibers requires a comprehensive understanding of the frequency-dependent behavior of fiber parameters such as attenuation and chromatic dispersion. For instance, in Standard Single-Mode Fiber (SSMF), the attenuation coefficient generally remains below 0.2 dB/km in the C-bands. Additionally, Stimulated Raman Scattering (SRS) is a nonlinear optical phenomenon that transfers power from higher-frequency signals to lower-frequency ones [26]. SRS has minimal impact in systems limited to the C-band.

The QoT for each channel within a span of optical fiber, indexed by i, can be evaluated using the Generalized Signal-to-Noise Ratio (GSNR), defined as:

$$\mathrm{GSNR}_i = \frac{P_{S,i}}{P_{ASE,i} + P_{NLI,i}} = \left(\mathrm{OSNR}_i^{-1} + \mathrm{SNR}_{\mathrm{NLI},i}^{-1}\right)^{-1} \tag{2.2}$$

Here: $P_{S,i}$ is the span input signal power, OSNR_i represents the optical signal-to-noise ratio, and $\text{SNR}_{\text{NLI},i}$ refers to the nonlinear signal-to-noise ratio.

This model assumes that the primary contributors to signal degradation are Amplified Spontaneous Emission (ASE) noise and Nonlinear Interference (NLI) noise, arising from optical amplifiers and fiber propagation, respectively. Both noise sources are approximated as Gaussian disturbances across a wide range of transmission scenarios. The ASE noise power $P_{ASE,i}$ is derived using established equations, while the nonlinear power contribution $P_{NLI,i}$ is determined via the Generalized Gaussian Noise (GGN) model [27]. The GGN model incorporates the effects of both spectral and spatial variations in fiber loss and SRS-induced inter-channel power crosstalk.

Within a disaggregated representation of the physical layer [28], the overall QoT for a lightpath l is determined by aggregating the inverse GSNR values across all fiber spans s traversed by the lightpath:

$$\text{GSNR}_{i,l} = \frac{1}{\left(\sum_{s\in l} \text{GSNR}_{i,s}^{-1}\right)^{-1}} \tag{2.3}$$

This method, as implemented in the open-source GNPy library [29], enables precise QoT estimation. Erbium-Doped Fiber Amplifiers (EDFAs) are utilized for the C-band.

2.5 Characterization of the network abstraction

The integration of DSP-based coherent transmission technologies, combined with advancements in optical amplifiers and ROADM systems, has revolutionized optical networking. These innovations enable the development of elastic and transparent optical networks within unified domains, significantly altering operational dynamics. The shift toward an all-optical network architecture offers greater flexibility, scalability, and efficiency by handling optical signals directly without the need for conversion to electrical signals for amplification or switching. A key enabler of this transformation is the introduction of transceivers capable of supporting hybrid modulation formats and adaptable rate adjustments. These transceivers empower networks to dynamically create and modify optical channels, allowing real-time adaptation to shifting traffic patterns. This adaptability ensures efficient bandwidth management and resource optimization based on current network demands. In WDM transport layers, understanding the constraints of the physical layer is critical for establishing LPs between network nodes. Achieving optimal performance requires a comprehensive evaluation of the network's physical parameters, particularly given the dynamic nature of optical channel design enabled by advanced transceivers. By determining the GSNR for each wavelength across single-band configurations, the network topology can be simplified into a weighted graph representation. In this abstraction, each link is assigned a weight corresponding to the GSNR value of its associated wavelengths, which acts as a quantitative measure of QoT across the network.

This approach simplifies the complexity of optical network topologies into a clear framework of light routes, each characterized by its GSNR value. A higher GSNR indicates superior signal integrity, reduced noise, and improved transmission quality, enabling higher data throughput. A practical method for RWA within this framework involves the use of waveplanes. Waveplanes serve as virtual representations of wavelengths available for transmission, providing a visual map of routing options. This visualization aids network engineers in selecting optimal routes for constructing light paths, taking into account factors such as latency, throughput, and network reliability.

The integration of optical network abstraction, leveraging GSNR values to assess light path quality and employing waveplanes for strategic RWA, provides a robust methodology for designing, analyzing, and optimizing the performance of high-speed optical networks.

Lightpath & Routing and wavelength assignment

A lightpath (LP), in optical networks, refers to a dedicated optical channel connecting two ROADMs or network nodes. Analogous to a circuit in electronic networks, LPs are essential for facilitating optical communication by providing a predefined path for light to traverse between nodes. This dedicated channel eliminates bandwidth contention, ensuring high network performance and reliability.

LPs are configured over specific wavelengths, utilizing WDM technology to multiplex multiple optical carrier signals on a single fiber by assigning different wavelengths of laser light. This approach allows simultaneous transmission of multiple signals over the same medium, greatly enhancing network capacity. In cases where spectral resources are constrained and no single wavelength is available across the entire path, the RWA algorithm optimizes resource usage. It may allocate the residual capacity of existing LPs that share the same source and destination nodes, maximizing spectral efficiency.

The importance in the optical networks management of Routing and Wavelength Assignment (RWA) is mainly due to its function of establishing connections between nodes. The RWA process consists of two stages: routing space calculation and wavelength assignments [30]. Essentially, these stages include the selection of an appropriate lightpath for data transmission by allocating spectral resources along a predefined path for the optical signal. The routing space computation is performed using the Dijkstra algorithm (also known as the k-shortest path approach) [31], which allows computing a set of k possible paths ordered from shortest in length to longest. The path selection process is conducted on a graph where weights are assigned to the edges, with these weights varying based on different metrics. As first metric it is possible to consider uniform weight. It assigns the same weight to all links, in order to balance network traffic. The aimed result is to minimize wavelength contention by reducing the number of ROADM nodes involved in the process. A second approach can consider as weight the GSNR degradation. An intelligent RWA strategy leveraging this metric optimizes GSNR along the paths, thereby enhancing the capacity and quality of each lightpath [32]. Alternatively, the physical length of the links is utilized as the weight, with a prioritization of the shortest path for the signal to travel. In this way is also possible to optimize the minimization of latency.

After the routing space computation, the next step involves assigning a specific wavelength for the connection. The most common strategies commonly employed are: Most-Used strategy and First-Fit strategy. The Most-used approach is predicated on the prioritization of wavelengths according to their frequency of usage within the network, with the most utilized wavelengths being given priority. Although this approach has the potential to optimize network resource utilization, the main negative impact is that it needs a comprehensive view of the network's overall wavelength usage. The First-Fit strategy is based on the consideration of wavelengths in ascending order of frequency, from lowest to highest. This method is preferred for its simplified approach and the fact that it does not necessitate a comprehensive understanding of network's current state.

In the domain of optical networks, wavelength assignment is constrained by several factors that ensure efficient and reliable operation. These constraints are essential for optimizing the utilization of network resources and maintaining the quality of transmission. The wavelength continuity constraint necessitates the utilization of a singular wavelength throughout the entirety of a lightpath. The uniformity of wavelength across all segments of the connection eliminates the necessity for wavelength converters, which, while augmenting flexibility, result in additional costs and complexity. By enforcing wavelength continuity, the RWA algorithm simplifies network design and operational management. It also ensures that the selected wavelength for any segment does not interfere with existing connections, enhancing bandwidth utilization and overall network performance. A further constraint pertains to wavelength contiguity, which guarantees that multiple wavelength channels are closely spaced in the optical spectrum, thereby circumventing substantial gaps. This configuration optimizes the utilization of available spectrum, facilitating higher data transmission rates and enhanced network performance. Furthermore, contiguous wavelength allocation streamlines wavelength management and simplifies allocation processes, thus empowering the network to address escalating data demands with greater efficacy.

The simulation software used, implement the RWA algorithm following these steps:

1. Pre-computation of the routing space,
2. when a new connection request is received, the algorithm seeks to allocate a lightpath, commencing from the shortest path and progressing to longer ones based on the first-fit wavelength availability strategy,
3. the allocation of the lightpath is contingent upon the availability of the necessary network resources and the determination of the feasibility of the chosen path, as determined by the signal quality. In the event that these conditions are not met, the connection request is to be denied.

Chapter 3

Simulation tools and traffic analysis

In order to meet the mounting demand for augmented optical network capacity and the necessity for cost-effective strategies, network operators must devise efficacious methodologies to enhance existing fiber infrastructure. It emphasizes the reliance on C-band WDM technology. Core networks are expected to face increasing pressure to support both higher capacity and greater flexibility as advanced technologies become more widespread at the network edge.

While current backbone networks effectively manage existing traffic demands, the anticipated surge in capacity needs-driven by on-demand applications will necessitate a significant transformation of network infrastructure. Ensuring continued progress in networking advancements requires a comprehensive understanding of present technologies, their limitations, and the innovations needed for future core networks.

The optical network layer, traditionally static, must evolve to accommodate dynamic service demands. Enhanced flexibility and rapid reconfiguration will be essential, not only for resource optimization but also for network restoration in the event of failures. As mission-critical applications increasingly rely on high-volume data transfers, the ability to withstand multiple simultaneous failures will be vital to ensuring uninterrupted service continuity. In order to address the aforementioned challenges, two primary strategies have emerged: Spatial Division Multiplexing (SDM) and Band Division Multiplexing (BDM).

SDM leverages the spatial properties of light by utilizing Multicore (MCF), Multimode (MMF), or Multiparallel (MPF) fibers to enhance the network's data-carrying capacity. However, this approach entails a comprehensive restructuring of the prevailing optical transport infrastructure, necessitating the integration of novel fiber types and the development of specialized apparatus tailored to this sophisticated architecture. In contrast, the objective of BDM is to expand the operational range of optical fibers by enabling low-loss transmission across a broader spectrum, encompassing the 54 THz bandwidth of ITU G.652.D fibers. A key benefit of BDM is its capacity to augment network capacity without necessitating additional optical fibers, thereby rendering it a more immediately viable option. The primary challenge associated with BDM pertains to optical amplification, which is imperative to meet the demands of the expanded spectrum. The development of prototype amplifiers capable of functioning within these expanded spectrum domains is a current priority. The successful implementation of BDM is contingent upon advancements in clear wavelength routing, necessitating the integration of advanced filtering and switching components tailored for this expanded operational range.

3.1 Simulation tools

3.1.1 GNPy

The Telecom Infra Project (TIP) is one of the key industrial consortia and standardization bodies focused on developing open networking solutions. TIP brings together network operators and vendors to create open software and hardware solutions for open networking. Within TIP, the Open Optical and Packet Transport (OOPT) working group specifically addresses multi-layer solutions for Open Optical Networking (OON), aligning with the partially disaggregated network architecture. Given that optical networking relies on WDM optical circuits deployed and routed over a transparent optical infrastructure, OON requires full virtualization of the physical layer to enable dynamic, software-defined optimization of optical networks. A notable initiative within this framework is the TIP project Gaussian Noise in Python (GNPy) [33], which aims to develop an open-source software model of the WDM transport layer. This model functions as a digital twin of the optical infrastructure, supporting network design, planning, and management operations.

The OOPT project GNPy is an open-source software effort that approximates transparent optical circuit (lightpaths) as additive white Gaussian noise (AWGN) channels, reflecting state-of-the-art dual-polarization coherent optical technologies. Through this abstraction, the physical layer is represented by the LP's Quality of Transmission (QoT), which is summarized by the Generalized Signal-to-Noise Ratio (GSNR). This metric accounts for key impairments such as Amplified Spontaneous Emission (ASE) noise from optical amplifiers and Nonlinear Interference (NLI) arising from fiber propagation. At the core of GNPy is a QoT estimator, which operates on the network's topological graph to compute the GSNR for a given wavelength and selected LP by cumulatively assessing QoT impairments across all traversed network elements. [34]

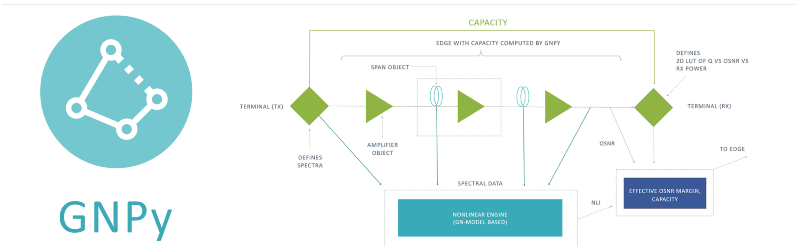

Figure 3.1: GNPy with an OLS system [35]

The key requirement for advancing open and disaggregated networking from demonstration to production environments is the availability of vendor-neutral design and planning tools. These tools enable network operators to virtually test and compare multi-vendor solutions during the network design phase, ensuring interoperability and optimal performance.

GNPy serves as a vendor-neutral design tool for optical networks, allowing operators to evaluate and benchmark different optical layer design solutions. To achieve this, vendors must provide GNPy compatible models for their network elements, enabling operators to leverage GNPy's simulation metrics to assess and challenge bidders' designs. Furthermore, these metrics can be integrated with techno-economic analyses to support cost-effective network planning.

Beyond its role in initial network planning, GNPy can also be utilized to virtually test potential network upgrades, providing a flexible and efficient approach to continuous network improvement [36].

GNPy uses a set of JSON files to model the network, organizing various types of data essential for accurate simulations. Some of these files define network topology, detailing nodes, links, and their characteristics, while others specify service requests, describing connection demands and their attributes. This structured approach enables GNPy to simulate real-world optical networks effectively, providing valuable insights into performance, capacity, and quality of transmission. Design and transmission parameters are specified in a dedicated JSON file, which serves as a central repository for defining network elements. This file includes customizable equipment libraries encompassing amplifiers, ROADMs, fibers, and transceivers. By adjusting these parameters, users can tailor the network model to reflect specific design choices, enabling more precise simulations and performance evaluations [37].

EDFA

The EDFA equipment library consists of a catalog of supported amplifiers, allowing users to customize their network configurations. New amplifier models can be added, while existing ones can be modified or removed as needed. Additionally, the library provides multiple noise models, enabling accurate representation of amplification effects within the optical network.

Field	**Type**	**Description**
type_variety	(string)	A unique name to ID the amplifier in the JSON/Excel template topology input file.
out_voa_auto	(boolean)	Auto-design feature to optimize the amplifier output VOA. If true, the output VOA is present and will be used to push amplifier gain to its maximum, within EOL power margins.
allowed_for_design	(boolean)	If false, the amplifier will not be picked by auto-design but it can still be used as a manual input (from JSON or Excel template topology files).
f_min and f_max	(number)	Optional. Minimum and maximum frequency range for the amplifier. Signal must fit entirely within this range (center frequency and spectrum width). Default is 191.275 THz and 196.125 THz.

Table 3.1: Amplifier Field Descriptions

Fiber

The fiber library currently includes descriptions for Standard Single-Mode Fiber (SSMF) and Non-Zero Dispersion-Shifted Fiber (NZDF). However, users can expand the library by adding additional fiber types, following the same modeling structure. This flexibility allows for tailored network simulations that accommodate a variety of fiber characteristics and transmission scenarios.

Field	**Type**	**Description**
type_variety	(string)	A unique name to ID the fiber in the JSONExcel template topology input file.
dispersion	(number)	In $s \times m^{-1} \times m^{-1}$.
dispersion_slope	(number)	In $s \times m^{-1} \times m^{-1} \times m^{-1}$.
disperison_per_frequency	(dict)	Dictionary of dispersion values evaluated at various frequencies.
effective_area	(number)	Effective area of the fiber (A_{eff}).
gamma	(number)	Coefficeint $\gamma = 2\pi \times n^2/(\lambda \times A_{eff})$.
pmd_coeff	(number)	Polarization mode dispersion (PMD) coefficient.
lumped_losses	(array)	Places along the fiber length with extra losses. Specified as a loss in dB at each relevant position.
raman_coefficient	(dict)	The fundamental parameter that describes the regulation of the power transfer between channels during fiber propagation is the Raman gain coefficient. Default values measured for a SSMF are considered when not specified.

Table 3.2: Fiber Field Descriptions

RamanFiber

The Raman Fiber enables the simulation of Raman amplification using dedicated Raman pumps. Each Raman pump description must include the following details:

Field	**Type**	**Description**
power	(number)	Total pump power in W considering a depolarized pump.
frequency	(number)	Pump central frequency in Hz.
propagation_direction	(number)	The pumps can propagate in the same or opposite direction with respect the signal. Valid choices are coprop and counterprop, respectively.

Table 3.3: Raman fiber Field Descriptions

In addition to the list of Raman pumps, the operational dictionary of the Raman Fiber must include the temperature that affects the amplified spontaneous emission noise generated by the Raman amplification. As the loss coefficient varies significantly outside the C-band, where the Raman pumps are usually placed, it is suggested that an estimation of the loss coefficient for the Raman pump central frequencies be included within a dictionary-like definition.

ROADM

The user can only modify the values of existing parameters, such as:

Field	Type	Description
type_variety	(string)	Optional. A unique name to ID the ROADM variety in the JSON template topology input file.
target_pch_out_db or target_psd_out_mWperGHz or target_out_mWperSlotWidth (mutually exclusive)	(number)	Auto-design sets the ROADM egress channel power. This reflects typical control loop algorithms that adjust ROADM losses to equalize channels. These values are used as defaults when no overrides are set per each ROADM element in the network topology.
add_drop_osnr	(number)	OSNR contribution from the add/drop ports.
pmd	(number)	Polarization mode dispersion.
restriction	(dict of strings)	If non-empty, keys preamp_variety_list and booster_variety_list represent list of type_variety amplifiers which are allowed for autodesign within ROADM's line degrees.
roadm-path-impairments	(list of dict)	Optional. List of ROADM path category impairments.

Table 3.4: ROADM Field Descriptions

Span

The span configuration is not a list, and the user can only modify the values of the existing parameters:

Field	Type	Description
power_mode	(boolean)	If **false**, gain mode: only gain settings are used for propagation. The gain mode is recommended if all the amplifiers have already consistent gain settings in the topology input file. If **true**, power mode. It is recommended for autodesign and power sweep.
deltapower_range_db	(number)	Auto-design only, power mode only. It specifies the $[min, max, step]$ power excursion/span.
max_fiber_lineic_loss_for_raman	(number)	Maximum linear fiber loss for Raman amplification use.
max_length	(number)	Interest to support high level topologies that do not specify in line amplification sites.
length_unit	m/km	Unit for max_length.
padding	(number)	In dB. Minimum span loss before putting an attenuator before fiber.
EOL	(number)	All fiber span loss ageing. The value is added to the fiber output connector; so the design and the path feasibility are performed with $span\_loss + EOL$
con_in, con_out	(number)	Default values if Fiber/params/con_in/out is None in the topology input description. This default value is ignored if a Fiber/params/con_in/out value is input in the topology for a given Fiber.

Table 3.5: Span Field Descriptions

Spectral Information

GNPy requires a comprehensive delineation of all channels that will be disseminated through the network. This block delineates a reference channel, which is employed for the design of the network or the correction of settings.

Field	Type	Description
type_variety	(string)	Optional. A unique name to ID the band for propagation or design.
f_min, f_max	(number)	In Hz. They define spectrum boundaries.
baud_rate	(number)	In Hz. Simulated baud rate.
spacing	(number)	In Hz. Carrier spacing.
roll_off	(number)	Pure number between 0 and 1. TX signal roll-off shape. Used by Raman-aware simulation code.
tx_osnr	(number)	In dB.OSNR out from the transponder.
power_dbm	(number)	In dBm. Target input power in spans to be considered for the design in gain mode, if no gain is set in an amplifier, auto-design sets gain to meet this reference power. If amplifiers gain is set, *power_dbm* is ignored.
tx_power_dbm	(number)	In dBm. Optional. Power out of the transceiver.
power_range_db	(number)	Power sweep excursion around *power_dbm*. This defines a list of reference powers to run the propagation. Power sweep is an easy way to find the optimal reference power. It is ignored in case of gain mode.
sys_margin	(number)	In dB. Added margin on min required transceiver OSNR.

Table 3.6: Spectral Information Field Descriptions

Transceiver

The transceiver equipment library contains a list of supported transceivers. Users have the flexibility to add new transceivers or remove existing ones as needed. This adaptability allows for customized network simulations that align with specific deployment requirements and technological advancements.

Field	**Type**	**Description**
type_variety	(string)	A unique name to ID the amplifier in the JSON/Excel template topology input file.
frequency	(number)	Min/max central channel frequency.
mode	(number)	A list of modes supported by the transponder. New modes can be added at will by the user. The modes are specific to each transponder type_variety.

Table 3.7: Transceiver Field Descriptions

Each mode is defined as depicted in Table 3.8

Field	**Type**	**Description**
format	(string)	A unique name to ID the mode.
baud_rate	(number)	In Hz.
OSNR	(number)	Minimum required OSNR in 0.1nm (dB).
bit_rate	(number)	In bit/s.
roll_off	(number)	Pure number between 0 and 1. TX signal roll-off shape. Used by Raman-aware simulation code.
tx_osnr	(number)	In dB. OSNR out from transponder.
equalization_offset_db	(number)	In dB. Deviation from the per channel equalization target in ROADM for this type of transceiver.
penalties	(list)	List of impairments as described in impairment table.
cost	(number)	Arbitrary unit.

Table 3.8: Transceiver's mode Field Descriptions

3.1.2 SNAP tool

GNPy provides as the physical layer QoT metric the GSNR. Now it is necessary to deal with the network layer, representing the network architecture as a weighted graph and using QoT as the weight for each link. This method of modeling facilitates a thorough evaluation of the network's configuration and its capacity for optimal functionality.

The Statistical Network Assessment Process (SNAP) tool is utilized for the purpose of conducting network analysis. SNAP focuses on assessing network performance, particularly its efficiency in capacity utilization. It conducts a detailed evaluation of network reliability and efficiency using precise QoT metrics, such as GSNR. The SNAP tool utilizes a comprehensive methodology for conducting a statistical analysis of network performance, leveraging a Monte Carlo (MC) simulation approach. This technique enables the evaluation of various network scenarios by simulating a wide range of possible conditions. By repeatedly sampling different configurations and traffic conditions, the MC simulation ensures an accurate estimation of key performance indicators, such as GSNR. This methodological framework empowers network operators to proactively identify and address potential challenges, optimize resource allocation, and enhance the overall resilience of the optical transport infrastructure.

The first stage of the process requires defining the essential input parameters necessary for the tool's operation. These parameters include a comprehensive representation of the network's physical layer, a traffic model, and the specific Routing and Wavelength Assignment (RWA) algorithm to be applied. The physical topology of the network is modeled as a weighted graph consisting of N_{nodes} and N_{links} edges, where nodes represent ROADMs, and edges denote the optical links interconnecting these nodes. Each edge is assigned a weight $w_{i,j}$, which serves as a quantitative measure of transmission impairments, incorporating both Amplified Spontaneous Emission (ASE) noise and Nonlinear Interference (NLI). These values are computed using GNPy's Quality of Transmission Estimator (QoT-E), ensuring an accurate assessment of optical signal quality across the network. The traffic model is structured as a $N_{\text{nodes}} \times N_{\text{nodes}}$ probability matrix, where each element $p_{i,j}$ represents the probability of a connection request occurring between nodes i and j. This probabilistic framework enables SNAP to generate connection requests in a stochastic manner, ensuring that the distribution of requests aligns with the predefined probabilities in the matrix. Notably, the probability of connection requests is not uniform across all node pairs and can be adjusted to reflect varying levels of demand between different network regions. Additionally, the model is designed to be independent of past request patterns, ensuring that each connection request is treated as a distinct event, allowing for a more flexible and dynamic representation of network traffic.

At the heart of SNAP's simulation process lies the execution of N_{MC} Monte Carlo (MC) iterations. Each iteration begins with a completely unallocated network, meaning that no Light Paths (LPs) are initially established. During each iteration, SNAP selects a connection request based on the predefined traffic model and attempts to allocate resources according to the chosen Routing and Wavelength Assignment (RWA) algorithm. These algorithms may include First-Fit (FF), Minimum GSNR, Maximum GSNR, or other strategic approaches. If the allocation is successful, the connection request is accepted, and the necessary network resources are reserved for the corresponding LP. These allocated resources remain committed for the entire operational duration of the network, ensuring efficient utilization of spectral capacity while maintaining the required Quality of Transmission (QoT). The LP's capacity is then determined based on its GSNR, with this value and other relevant data systematically recorded for analysis. If the RWA algorithm finds that a connection request cannot be accommodated due to resource constraints, the request is rejected and logged as a blockage. The process continues with the generation and evaluation of additional connection requests until the network reaches a saturation point, which is defined by pre-established thresholds for blocking probability and the total number of requests. This entire procedure is repeated over N_{MC} Monte Carlo iterations, with the results averaged to generate a comprehensive set of performance metrics. These metrics provide valuable insights into the network's efficiency, capacity utilization, and overall reliability under various traffic conditions. The SNAP workflow is illustrated in Fig. 3.2

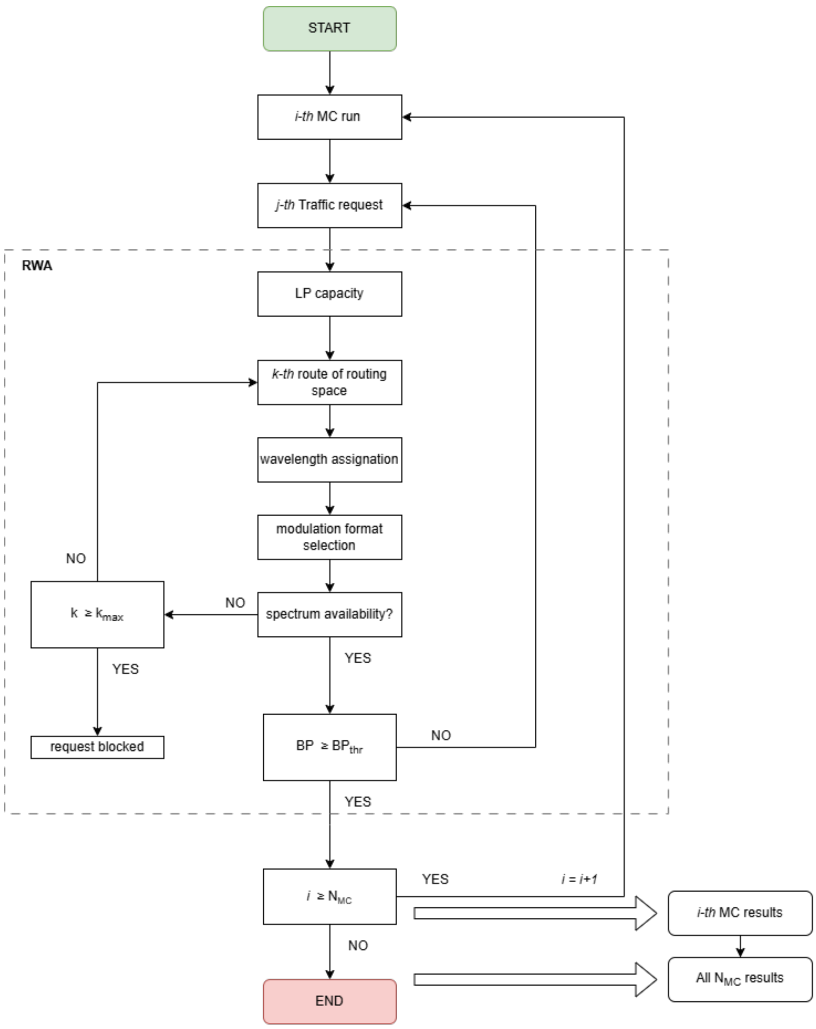

Figure 3.2: SNAP framework

3.2 Network topologies

In this study, the network topology of USA, Fig. 3.3, Europe, Fig. 3.4, and Germany, Fig. 3.5 have been utilized as the underlying framework for analysis. This topologies were chosen for their comprehensive representation of a real-world, large-scale optical network, providing valuable insights into the behavior and performance of optical systems under realistic operational conditions. The detailed structure of these networks, including transceivers, ROADMs, and fiber links, enabled the development and testing of various algorithms and network configurations, contributing to the depth and applicability of the findings in this research.

The network topology characteristics are summarized in the following table:

Topology	# of nodes	# of links	Average node degree	Average link length
USA	24	43	3.58	660 km
Europe	28	41	2.93	531 km
German	17	26	3.06	207 km

Table 3.9: Topologies characteristics

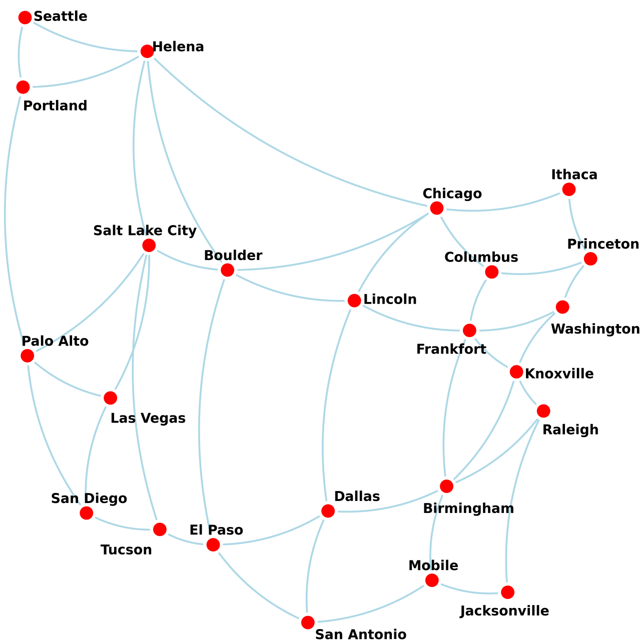

Figure 3.3: USA topology

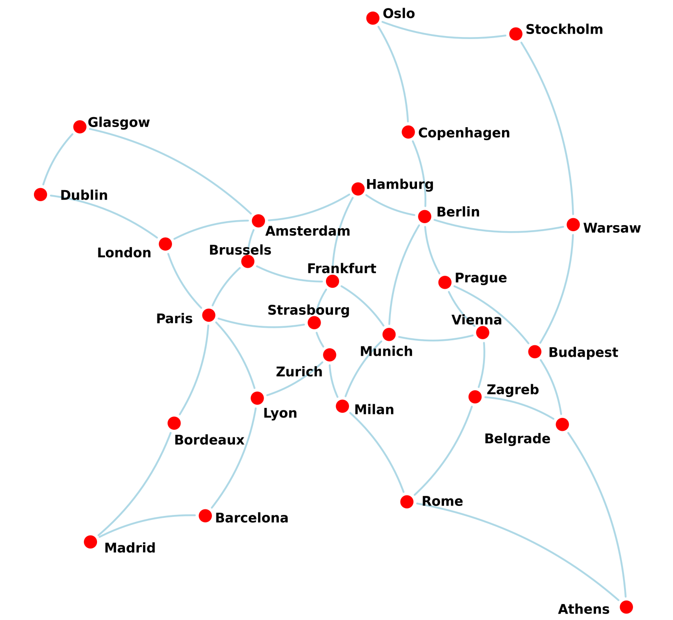

Figure 3.4: European topology

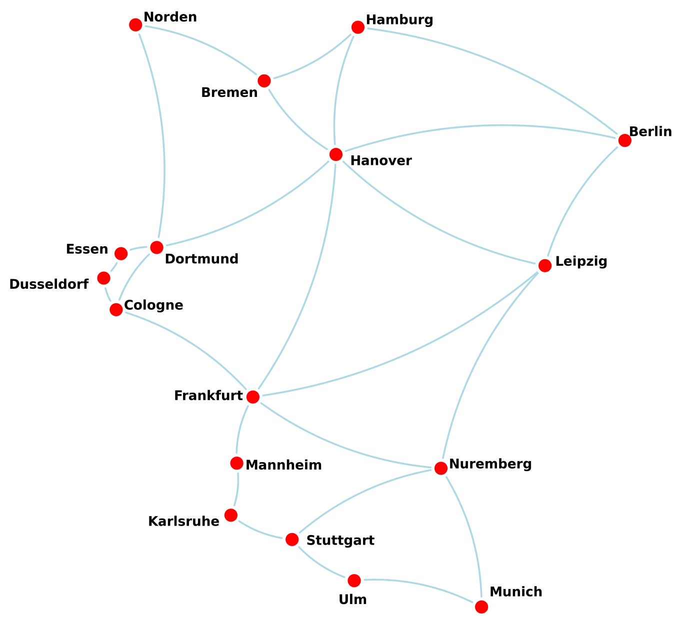

Figure 3.5: German topology

This study employs a detailed span-by-span approach to strategically optimize input power across the C optical bands. Today, optical fibers exhibit their lowest attenuation in the C-band, making it the most widely used spectral range for metro, long-haul, ultra-long-haul, and submarine optical transmission systems, especially when combined with Wavelength Division Multiplexing (WDM) and Erbium-Doped Fiber Amplifier (EDFA) technologies [38]. The C-band covers the wavelength range of 1530 – 1565 nm, which corresponds approximately to a frequency range of 191.5 THz to 196.25 THz. The Local Optimization Global Optimization (LOGO) algorithm is utilized to significantly enhance the Quality of Transmission (QoT) throughout the network. The Gain to Signal-to-Noise Ratio (GSNR) profiles for each band configuration are analyzed over a standard 75 km fiber span, considering them as functions of frequency. The interaction between different bands becomes evident through variations in GSNR profiles, which arise from the distinct gain and noise characteristics of the amplifiers operating within each band. Achieving a balanced GSNR across bands requires navigating a trade-off between amplifier gain profiles and optical power levels. While increasing amplifier gain can improve GSNR, it may also introduce additional Amplified Spontaneous Emission (ASE) noise, potentially degrading overall signal quality

3.3 Disaggregated optical networks

In this thesis, many commercial transceivers (TRXs) are used to perform network analysis. The main characteristics of the TRXs under study are described in Tab.3.10.

Parameter	**100G**	**200G**	**300G**	**400G**
Data Rate	100 Gbps	200 Gbps	300 Gbps	400 Gbps
Operating Distance	L > 2500 km	1500 < L < 2500 km	450 < L < 1500 km	120 < L < 450 km
Modulation	QPSK	QPSK	8QAM	16QAM
Power Consumption	∼ 13 W	∼ 16 W	∼ 18 W	∼ 20 W
Spectral Efficiency (BW=50GHz)	2 bit/s/Hz	4 bit/s/Hz	6 bit/s/Hz	8 bit/s/Hz
Spectral Efficiency (BW=100GHz)	1 bit/s/Hz	2 bit/s/Hz	3 bit/s/Hz	4 bit/s/Hz
Standards	IEEE 802.3ba [39]	IEEE 802.3bs [40]	OpenROADM MSA [41]	IEEE 802.3bs, OpenZR+ [42]

Table 3.10: TRXs parameters

Further simulation parameters are showed in Table 3.11:

Parameters	Value
# of iterations	1000
Traffic request	random 400-600 Gbps and random 400-1200 Gbps
Traffic distribution	Uniform
Type of fiber	Standard Single Mode Fiber (SSMF)
Network topology	USA (USNET), Europe (COST), and German (DT)
Number of channels	40
Channel spacing	100 GHz

Table 3.11: Simulation parameters

In the next Section, the simulation results for each topology will be presented.

3.4 Performance analysis of disaggregated optical networks

3.4.1 USNET

In this section will be reported the simulation results concerning the American (USNET) topology (Fig. 3.3). The approaches that have been utilized are: configuration with only 100G transceivers; configuration with only 200G transceivers; configuration with only 300G transceivers; configuration with only 400G transceivers; configuration with an adaptive transceiver selection.

The results are reported through a blocking probability vs allocated traffic chart representing the network capacity.

100G transceiver

In Fig.3.6 is depicted the behavior of the blocking probability for the USA network topology. Considering, as threshold to assess the traffic handling capacity, a blocking probability of 10^{-2} it is possible to notice a delivery capacity of about 23 Tbps considering only the 100G transceivers indicated in Tab. 3.10.

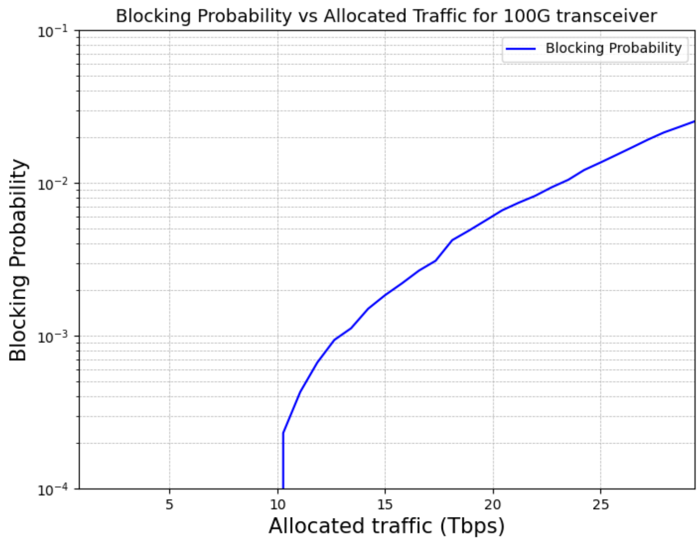

Figure 3.6: 100G transceiver: Blocking probability vs allocated traffic

200G transceiver

Fig. 3.7 shows that using 200G transceivers the network is able to handle about 61 Tbps of traffic. It is evident that this configuration presents an enhanced capacity with respect to the one using 100G transceivers.

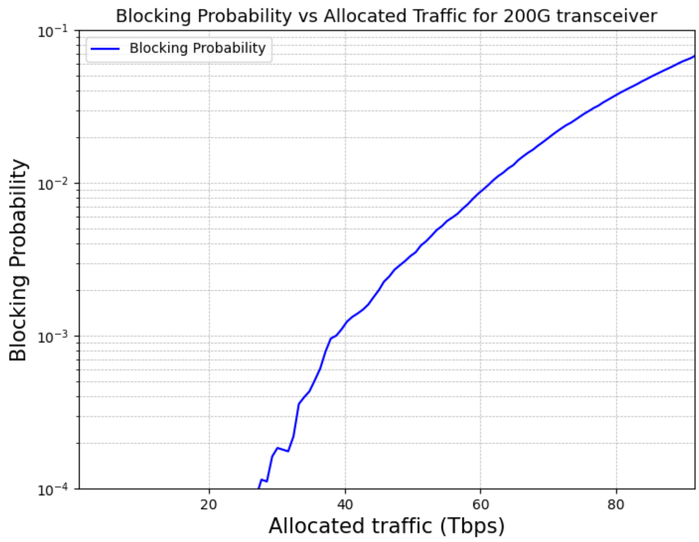

Figure 3.7: 200G transceiver: Blocking probability vs allocated traffic

Comparison

For the USNET network topology is not possible to use configurations containing only 300G or 400G transceivers. This is due to the fact that the link length of this topology does not match the operating distance of the transceivers. In fact, the SNAP tool does not provide any result since the traffic request are rejected. The SNAP tool offers the possibility to use a configuration containing multiple transceivers, able to automatically select the best transceiver for each link. In Fig. 3.8 it is possible to see the performance of this configuration. It is possible to detect a traffic capacity of about 74 Tbps. In table 3.12 it can be noticed the fact that the 200G and multiple transceivers approaches have similar performance in terms of traffic allocation, enhancing respectively of 126% the allocation of 100G solution and of 21% the allocation of the 200G one. Fig. 3.9 illustrates the average usage of the transceivers in the Monte Carlo simulations. The SNAP tools uses the transceivers in a distance based way. It is possible to denote: the high employment of 300G transceiver (380), a similar usage of the 200G (283) and 400G (269) transceivers, and the null usage of the 100G transceiver.

100G	200G	Multiple transceivers
23 Tbps	61 Tbps (+ 126%)	74 Tbps (+ 21%)

Table 3.12: Traffic allocation for USNET topology

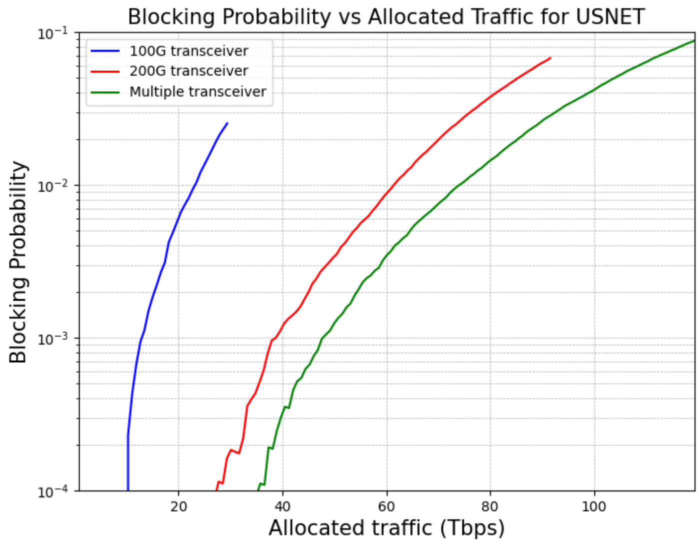

Figure 3.8: Comparison of the configurations

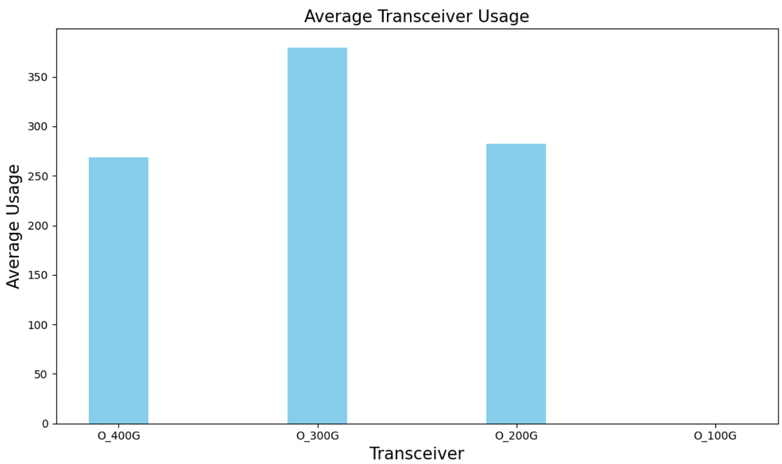

Figure 3.9: Average transceiver usage in the simulations

3.4.2 COST

In this section, the same result methodology described in 3.4.1 is adopted. In this case the considered topology is the European (COST) (Fig. 3.4).

100G transceiver

Fig. 3.10 illustrates the blocking probability vs traffic allocated behavior for the European (COST) topology. It is possible to recognize a 17 Tbps traffic allocation under the blocking probability (BP) threshold fixed at 10^{-2}.

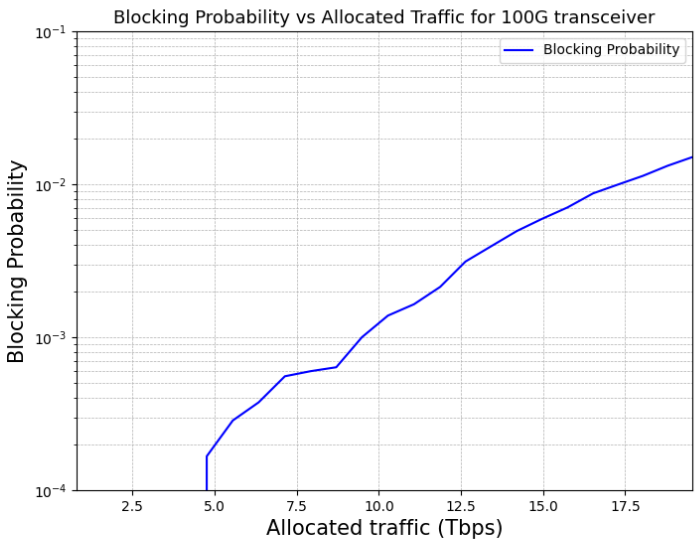

Figure 3.10: 100G transceiver: Blocking probability vs allocated traffic

200G transceiver

The 200G transceiver configuration, depicted in Fig. 3.11, allows a traffic allocation of over 47 Tbps under the BP threshold. It shows a consistent improvement with respect to the previous configuration.

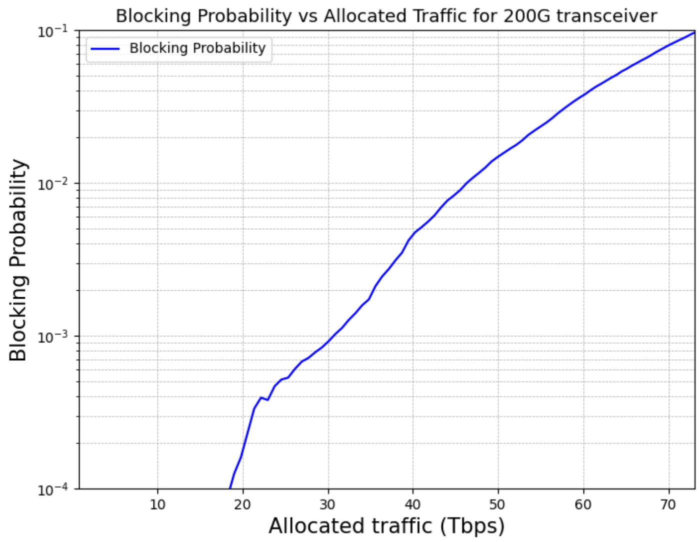

Figure 3.11: 200G transceiver: Blocking probability vs allocated traffic

Comparison

In the COST topology, as in the USNET, it is not possible to employ a configuration containing only 300G or 400G transceiver. This is caused by the fact that link length of the topology does not match the operating distances of the transceivers.

The dynamic transceiver selection of the SNAP tool is summarized in figure 3.12, underlining the fact that multiple transceiver configuration is the better choice in terms of traffic allocated. This configuration allows to reach a traffic allocation of 72 Tbps, 53% higher than the 200G solution, as reported in 3.13. A further analysis concerns the average transceiver usage across Monte Carlo simulations. Fig. 3.13 shows the result of this analysis and it is possible to detect the massive use of 300G (402) and 400G (433) use, the lower employment of 200G transceiver (69), while the 100G transceiver is not utilized.

100G	**200G**	**Multiple transceivers**
17 Tbps	47 Tbps (+ 176%)	72 Tbps (+ 53%)

Table 3.13: Traffic allocation for COST topology

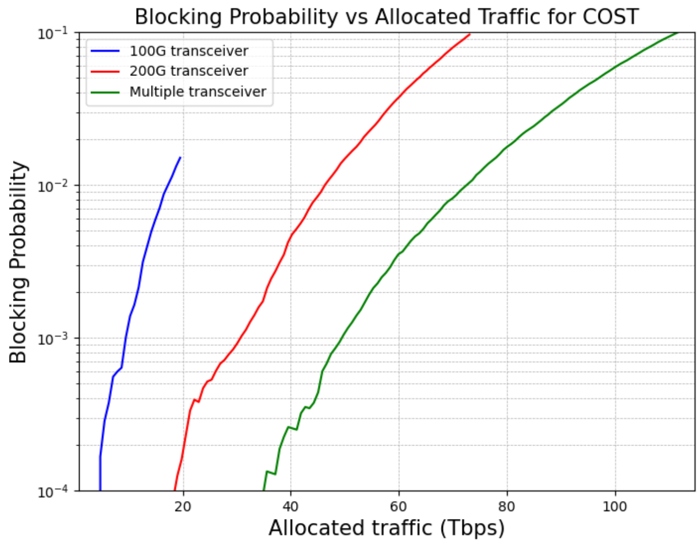

Figure 3.12: Comparison of the configurations

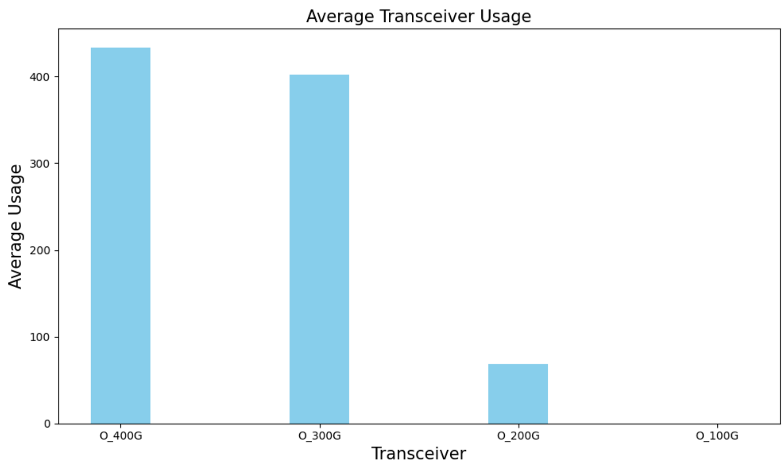

Figure 3.13: Average transceiver usage in the simulations

3.4.3 DT

In this section, the methodology described in Section 3.4.1 is adopted to evaluate the results. In this case the German topology (DT) (Fig. 3.5) is investigated. This topology permits to evaluate also the cases using only the 300G or 400G transceivers, since they do not cause blocking in the simulations.

100G transceiver

In Fig. 3.14, the blocking probability vs allocated traffic of the DT topology with only 100G transceivers configuration is represented. The traffic allocated considering a BP threshold of 10^{-2} is about 18 Tbps.

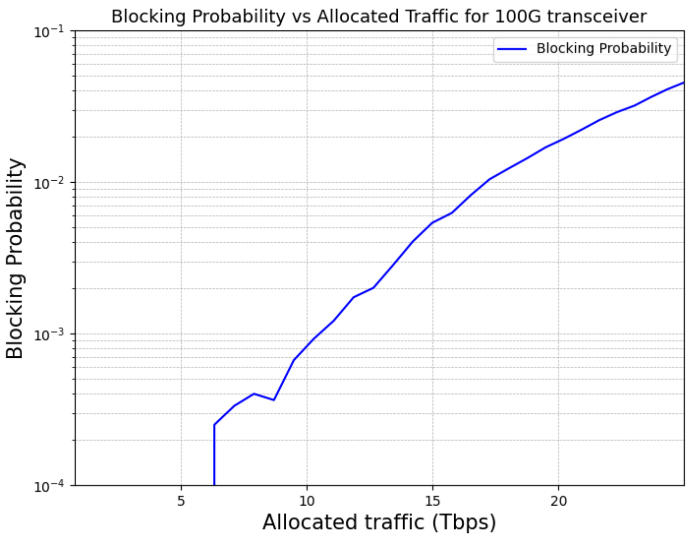

Figure 3.14: 100G transceiver: Blocking probability vs allocated traffic

200G transceiver

Figure 3.15 shows the behavior of the 200G configuration. In this case, the traffic allocation exceeds 44 Tbps, doubling that of the 100G configuration.

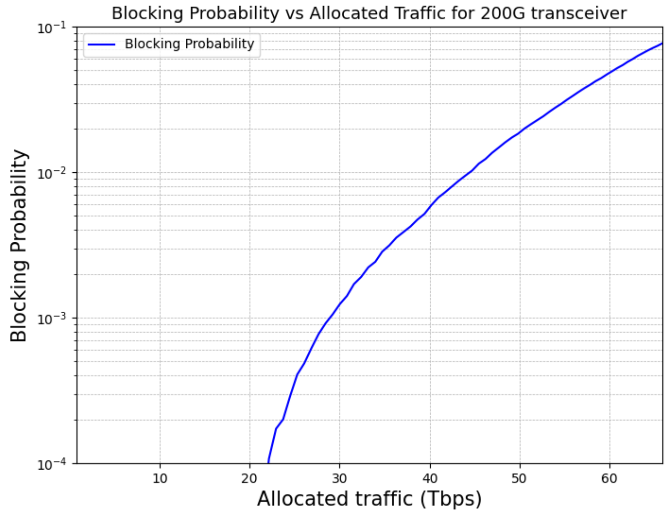

Figure 3.15: 200G transceiver: Blocking probability vs allocated traffic

300G transceiver

DT topology, due to the link length (Tab. 3.11), allows the 300G and 400G configurations. The smaller dimensions match the operational distances of all the transceivers considered. Figure 3.16 depicts the capability of the 300G network configuration. The traffic allocation, with BP under the considered threshold, is about 72 Tbps.

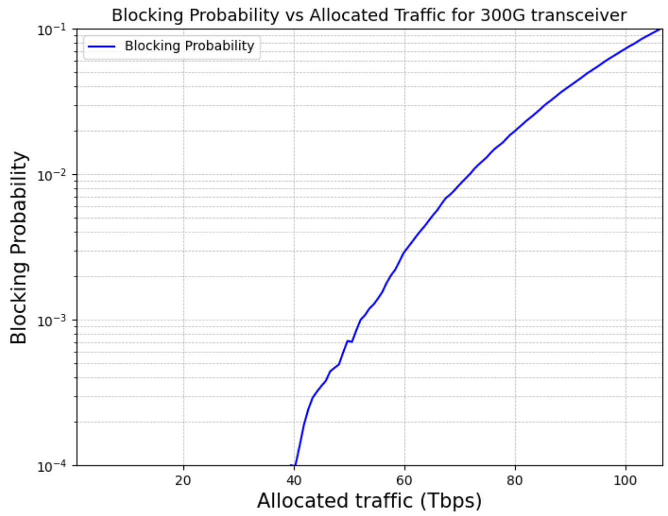

Figure 3.16: 300G transceiver: Blocking probability vs allocated traffic

400G transceiver

The performance of the 400G configuration is illustrated in Figure 3.17. The outcoming traffic allocation is of 94 Tbps, improving the 300G results.

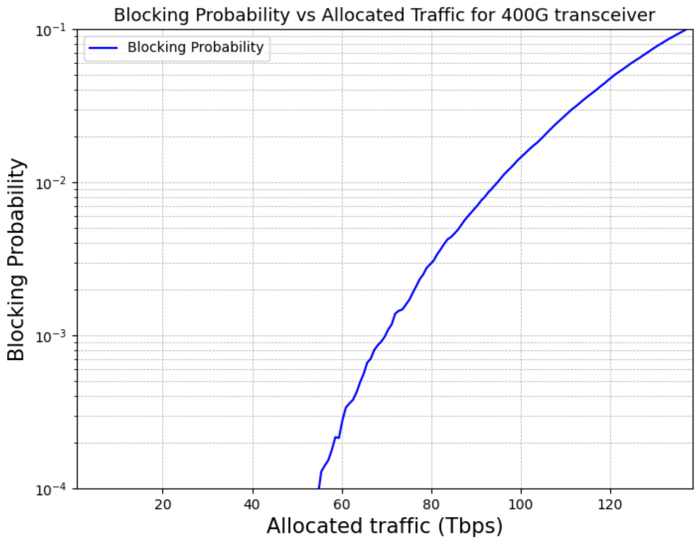

Figure 3.17: 400G transceiver: Blocking probability vs allocated traffic

Comparison

Fig. 3.18 displays the behavior of the multiple transceiver results performed by the SNAP tool. Figure 3.18 clearly shows the close performance among 400G and multiple transceivers configurations in the German topology. These scenarios exhibits a 31% increase in traffic allocation compared to the 300G scenario. The total traffic allocated, considering the BP threshold, is of about 94 Tbps (Table 3.14).

The average transceiver usage is demonstrated in Figure 3.19. This result is identical to the one obtained when employing only 400G, as the SNAP tool exclusively used 400G transceivers(882).

100G	200G	300G	400G	Multiple trxs
18 Tbps	44 Tbps (+ 144%)	72 Tbps (+ 63%)	94 Tbps (+ 31%)	94 Tbps

Table 3.14: Traffic allocation for DT topology

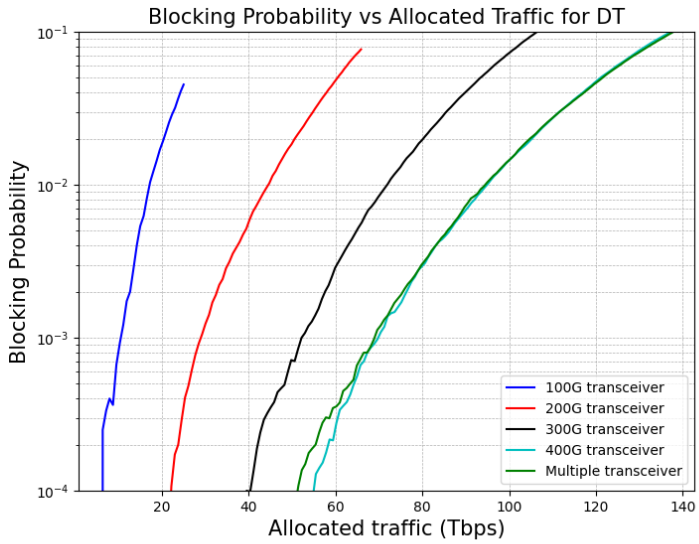

Figure 3.18: Comparison of the configurations

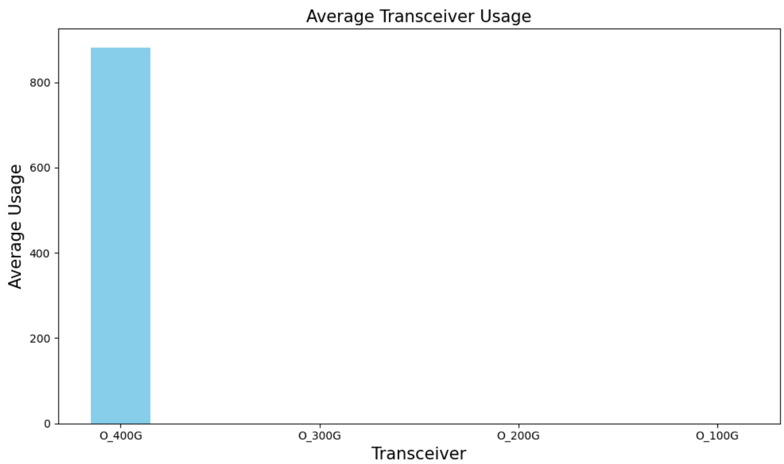

Figure 3.19: Average transceiver usage in the simulations

Chapter 4

Encrypted enabled transceivers

4.1 Background

Security is a critical component of modern networks, with operators constantly addressing a wide range of threats. Networks incorporate numerous functions to mitigate security risks, such as control management, denial of service (DoS) attacks, unauthorized access, and other vulnerabilities [43].

Layer 1 encryption solutions are extensively employed in regional, national, and international Dense Wavelength Division Multiplexing (DWDM) systems. Encrypting traffic at the physical network layer ensures that all data transmitted over the optical link is protected, offering an efficient and cost-effective method to safeguard sensitive information against attacks targeting the fiber infrastructure [44].

A robust encryption scheme provides multiple layers of protection [45]:

1. Confidentiality: Unauthorized reading of data is prevented through encryption mechanisms.

2. Integrity: Data alteration is prevented via digital signatures.

3. Authenticity: Replay attacks are mitigated by uniquely marking data packets (e.g., using counters or sequence numbers).

The Advanced Encryption Standard (AES) is a symmetric encryption system established in 2000 by the National Institute of Standards and Technology (NIST) as the successor to the Data Encryption Standard (DES). AES utilizes a block size of 128 bits and supports key lengths up to 256 bits. The encryption process involves multiple rounds in which the binary plaintext is combined with cryptographic keys and repeatedly transformed. AES is resistant to both linear and differential cryptanalysis, thereby providing strong protection for transmitted data.

Encryption at Layer 1 of the OSI model enables secure data transmission that is independent of the protocols and applications in use. This approach allows for the secure encryption of various types of traffic, including voice, data, and video, as well as multiple protocols such as Ethernet, Fibre Channel, Serial Digital Interface (SDI), and Common Public Radio Interface (CPRI) [45].

Optical networks support all communications traffic and cover the widest geographic areas, making them susceptible to attacks at multiple points. Layer 1 encryption serves as the foundational layer for securing optical networks, especially amid growing concerns about quantum computing's potential to break current public key-exchange algorithms. This type of encryption is a powerful tool for future-proofing networks against unauthorized intrusions and is particularly attractive to businesses because it does not introduce latency or performance overhead [46].

Layer 1 encryption is increasingly becoming the fundamental layer for safeguarding communications networks. In response to evolving cybersecurity threats and several large-scale breaches, new regulations are pressuring organizations to protect not only data centers and other forms of stored data but also data in transit across existing network infrastructures.

Figure 4.1 shows the different layers of encrytpion in the OSI model and how each level applies encryption.

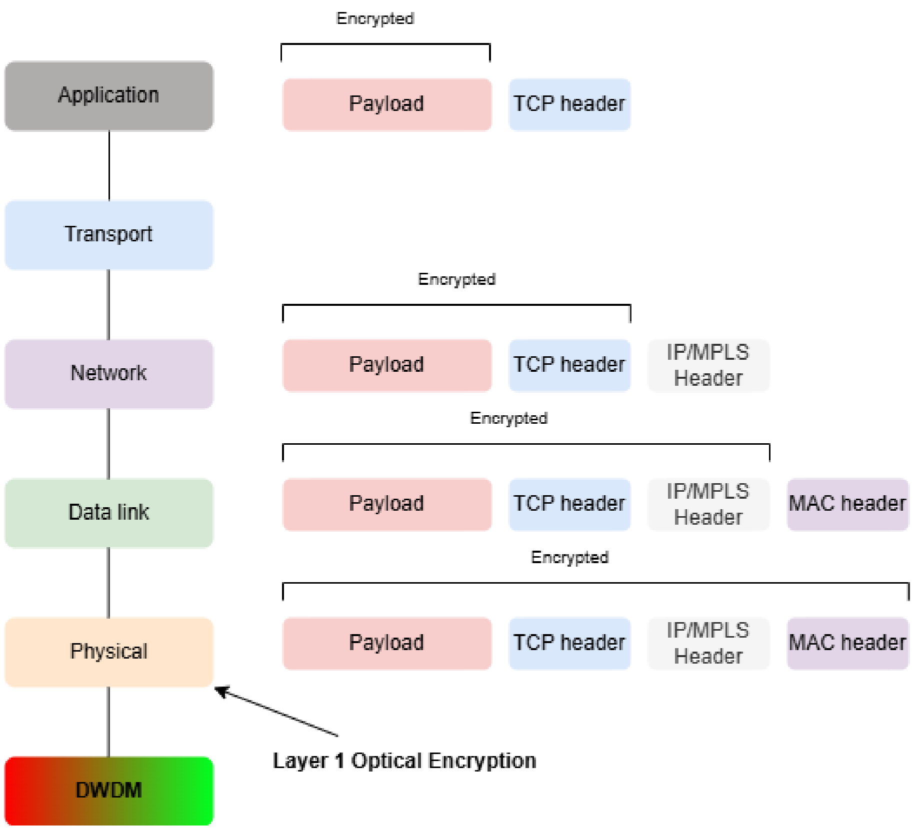

Figure 4.1: Levels of encryption

In this thesis, Layer 1 encryption is investigated, considering the three topologies mentioned in Chapter 3 and a 15% overhead impacting the transceivers bitrate in the simulations. Moreover, each topology contains an amount of about 25-30% randomly selected transceivers equipped for encryption. In the following section, each topology results will be illustrated, and compared with the unencrypted results.

4.2 Traffic analysis for encrypted enabled transceivers

4.2.1 USNET

Figure 4.2 displays the comparison in the blocking probability vs traffic allocation for both the encrypted and unencrypted approaches in the USNET topology. In this topology, the 30% of nodes are employed for the encryption: Palo alto, Salt Lake City, El Paso, Dallas, Birmingham, Ithaca, and Knoxville. As expected, the traffic allocation of unencrypted communication (74 Tbps) is higher than the encrypted one (72 Tbps). It is possible to note that the difference between the two strategies is of the 3 % even if the bitrate of each transceiver used is 15 % lower.

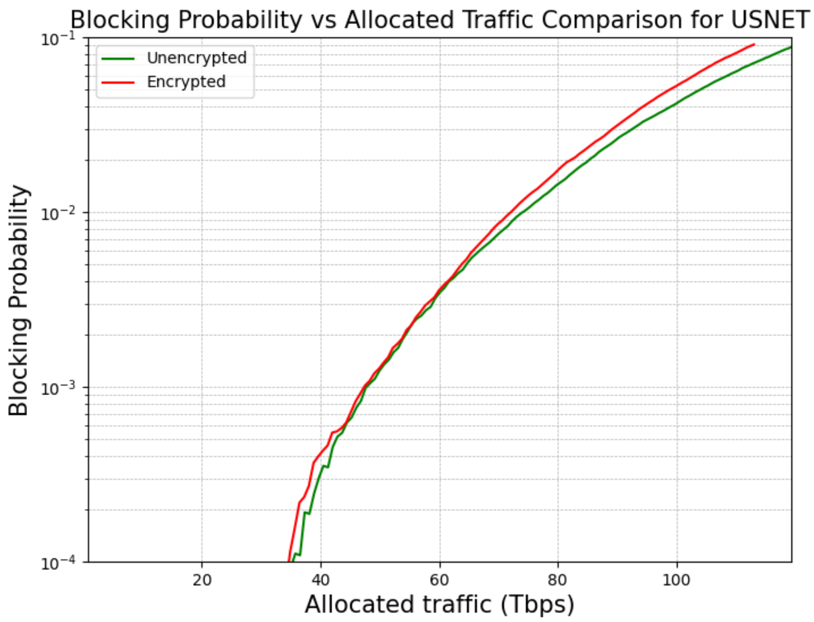

Figure 4.2: Multiple transceiver: Blocking probability vs allocated traffic comparison

4.2.2 COST

In the COST topology simulation, the 25% of nodes are used for the encryption. These nodes are: Brussels, Athens, Lyon, Zagreb, Prague, Oslo, and Vienna. The comparison for the COST topology is depicted in figure 3.12. The chart shows a clearer reduction in the traffic allocation in the encryption technique with respect to the non encrypted one. In the original approach the traffic allocation was of 72 Tbps, the encrypted solution reaches 65 Tbps, meaning in a drop of about 10 % of traffic.

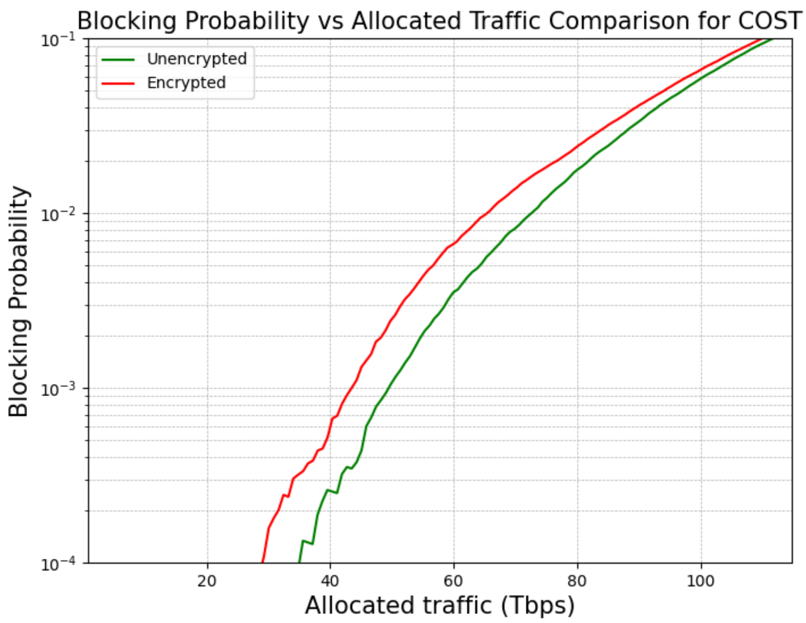

Figure 4.3: Multiple transceiver: Blocking probability vs allocated traffic comparison

4.2.3 DT

The German topology performance with the encryption traffic is displayed in figure 3.18. In this topology, the 30% of nodes are used for the encryption. The nodes where encrypted transceivers are placed are: Dortmund, Frankfurt, Cologne, Norden, and Stuttgart. The traffic allocation in this case is of 90 Tbps. Comparing this result with the one obtained in 3.4.3 (94 Tbps), the traffic decrease in the German topology amounts to 4 %. This result is similar to the one obtained in the USNET topology.

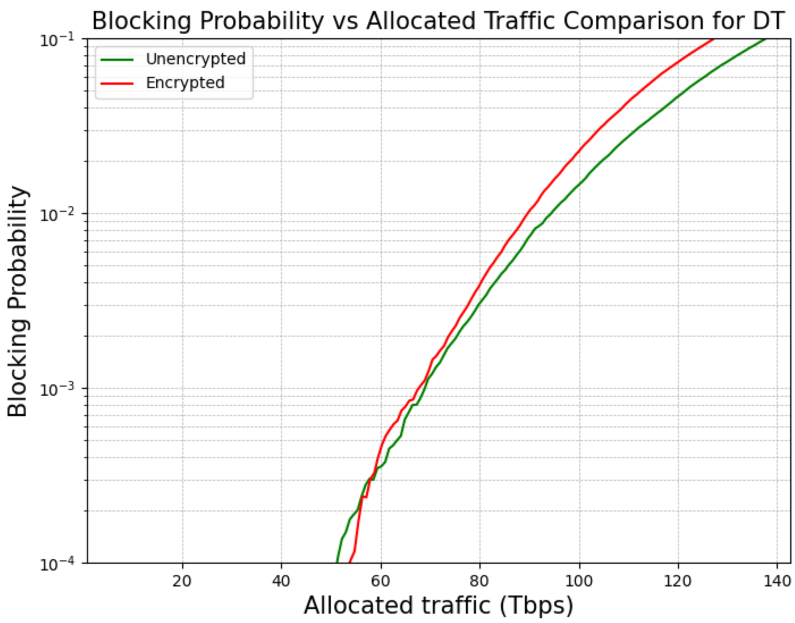

Figure 4.4: Multiple transceiver: Blocking probability vs allocated traffic comparison

4.3 Final results

In Table 4.1 all the results obtained are summarized. It can be noticed that COST topology is the one which gets less advantages in terms of traffic allocation, about 10 % of traffic is lost, using the Layer 1 encryption. On the other hand, encryption gets good results in the COST and DT topologies, with a minimal loss respectively of 3 % and 4 % of traffic allocation.

	USNET	**COST**	**DT**
Unencrypted	74 Tbps	72 Tbps	94 Tbps
Encrypted	72 Tbps	65 Tbps	90 Tbps
% encryption loss	3%	10%	4%
% of encrypted nodes	30%	25%	30%

Table 4.1: Comparison unencrypted vs. encrypted

In Figures 4.5, 4.6, and 4.7 the three topologies are showed; in these figures it is possible to notice, highlighted in blue, the nodes where encryption enabled transceivers are placed.

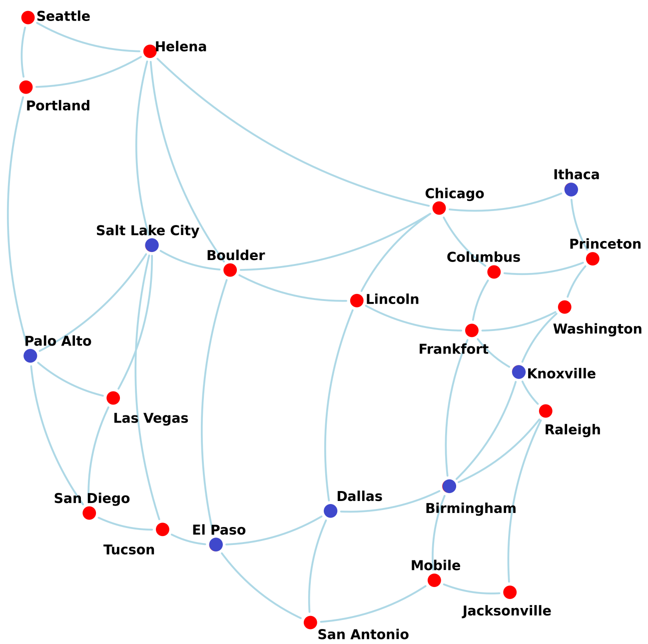

Figure 4.5: USNET topology with encryption enabled transceivers

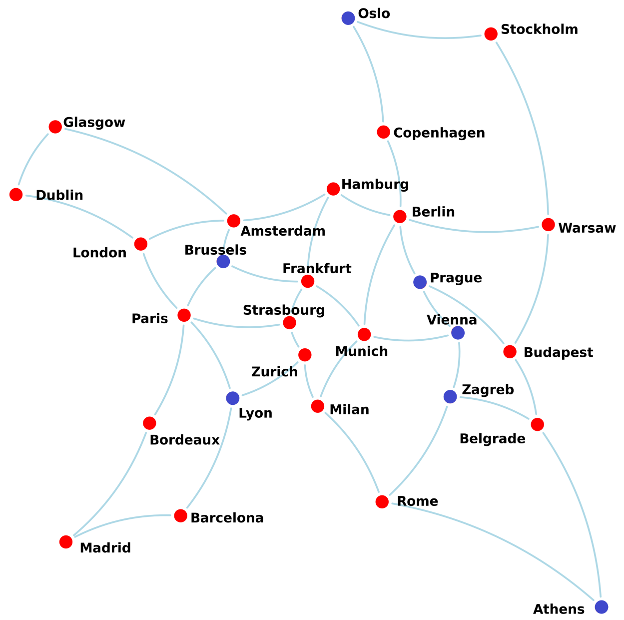

Figure 4.6: COST topology with encryption enabled transceivers

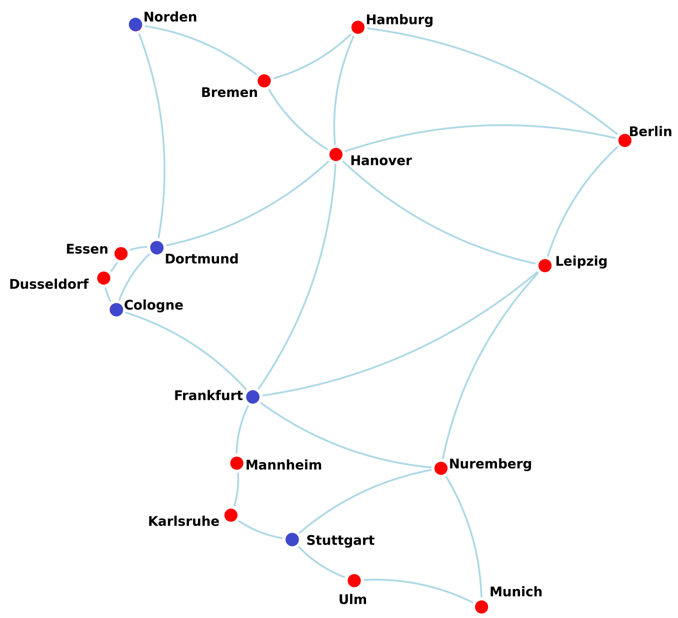

Figure 4.7: DT topology with encryption enabled transceivers

Chapter 5

Conclusion

In this final chapter, all the results obtained are summarized. In this study, it is possible to determine

In the first stage, the main goal was to compare the performance of different transceivers in the three network topologies. The methods under study include different configurations: structures comprehending only 100G, 200G, 300G, or 400G transceivers and a setup where the transceiver is dynamically selected on the basis of the distance between the nodes.

Table 5.1 shows the traffic allocation for each topology considering a blocking probability threshold of 10^{-2}.

	100G	**200G**	**300G**	**400G**	**Multiple trxs**
USNET	23 Tbps	61 Tbps	/	/	74 Tbps
COST	17 Tbps	47 Tbps	/	/	72 Tbps
DT	18 Tbps	44 Tbps	72 Tbps	94 Tbps	94 Tbps

Table 5.1: Summary of the results

As it is possible to deduce from the table, in every topology the configuration with adaptive transceiver allocation allows an higher traffic allocation. Notably, the DT topology shows that the allocation obtained by the 400G transceiver configuration has the same performance of the multiple transceiver approach and a very improvement in the total traffic allocation. Comparing all the multiple transceivers setups in all the topologies, the German network allows an improvement of about 30% in terms of traffic allocated. Moreover, in the USNET and COST topologies it is impossible to leverage on single 300G or 400G transceiver configurations; this result is due to the fact that the simulations encounter blocking requests caused by the mismatch of some link length with the operational distances of the transceivers (showed in Table 3.10).

A second analysis has been performed considering only the adaptive transceiver allocation for each topology. In this case, the number of transceiver used in each configuration is investigated.

	100G	**200G**	**300G**	**400G**
USNET	0	283 (30%)	380 (41%)	269 (29%)
COST	0	69 (8%)	402 (44%)	433 (48%)
DT	0	0	0	882 (100%)

Table 5.2: Transceiver usage in multiple trxs configurations

Table 5.2 displays the average transceiver usage in the multiple transceivers configuration in each topology.

In the USNET topology it can be identify an heterogeneous use of the 200G, 300G, and 400G transceivers, with the peak of 380 (41%) of 300G transceivers employed, while the 100G transceivers are completely unused. The COST topology, shows that the most employed transceivers are the 300G (44%) and the 400G (48%); in contrast with the USNET topology the 200G use is decreased until the 8 % of the total. In the DT topology, it is noticed the exclusive use of 400G transceivers; for this reason the German topology achieves the best performance in terms of traffic allocation.

The final analysis proposed regards the Layer 1 encryption. In this analysis, the impact of encryption on the traffic allocated by the multiple transceivers configurations is investigated. A random percentage of transceivers in each topology has been considered as encryption capable, with a 15% overhead impacting on the bitrate of each transceiver.

For the USNET topology, 30% of nodes are employed for encryption; they lead to a minimal loss (3%) in terms of allocated traffic; in the COST topology the encryption nodes amount to 25% and introduces a bigger loss, around 10% with respect to the unencrypted configuration; the DT topology reacts better to the encryption with a loss of about 4%.

The contrasting behavior of the COST topology can be explained by the fact that the encryption nodes act as bottlenecks in this configuration, leading to consistent losses. In figures 4.5, 4.6, and 4.7, the position of encryption enabled transceivers is highlighted. Table 5.3 summarizes the results of this analysis.

	USNET	**COST**	**DT**
% encryption nodes	30%	25%	30%
% encryption loss	3%	10%	4%

Table 5.3: Results of encryption

Bibliography

[1] Ramon Casellas, Ricardo Martinez, Ricard Vilalta, and Raul Munoz. Metro-haul: Sdn control and orchestration of disaggregated optical networks with model-driven development. In *2018 20th International Conference on Transparent Optical Networks (ICTON)*, pages 1–4. IEEE, 2018.

[2] Yoshihisa Yamamoto and Tatsuya Kimura. Coherent optical fiber transmission systems. *: IEEE Journal of Quantum Electronics 17.6*, pages 919–935, 1981.

[3] Jane M. Simmons. In *Optical network design and planning.* Springer, 2014.

[4] Kumar Sivarajan Rajiv Ramaswami and Galen Sasaki. Optical networks: a practical perspective. In *Morgan Kaufmann*, 2009.

[5] Derek Nesset. Next generation pon technologies: 50g pon and beyond (invited). In *2023 International Conference on Optical Network Design and Modeling (ONDM)*, pages 1–6, 2023.

[6] G. Kramer and G. Pesavento. Ethernet passive optical network (epon): building a next-generation optical access network. *IEEE Communications Magazine*, 40(2):66–73, 2002.

[7] T.D. Nadeau and K. Gray. *SDN: Software Defined Networks: An Authoritative Review of Network Programmability Technologies.* O'Reilly Media, 2013.

[8] ONF. Software-defined networking (sdn) definition. https://opennetworking.org/sdn-definition.

[9] A. Nayyar, B. Singla, and P. Nagrath. *Software Defined Networks: Architecture and Applications.* Wiley, 2022.

[10] Bruno Astuto A. Nunes, Marc Mendonca, Xuan-Nam Nguyen, Katia Obraczka, and Thierry Turletti. A survey of software-defined networking: Past, present, and future of programmable networks. *IEEE Communications Surveys and Tutorials*, 16(3):1617–1634, 2014.

[11] Bhawna Singla Anand Nayyar, Preeti Nagrath. *Software Defined Networks: Architecture and Applications.* Wiley-Scrivener, 1 edition, 2022.

[12] Alan E. Willner Ivan P. Kaminow, Tingye Li. *Optical Fiber Telecommunications. Volume VIB: Systems and Networks VIB.* Optics and photonics. Elsevier / Academic Press, 6 edition, 2013.

[13] Xiang Liu. Evolution of fiber-optic transmission and networking towards the 5g era. *iScience*, 22, 11 2019.

[14] Han Sun, Kuang-Tsan Wu, and Kim Roberts. Real-time measurements of a 40 gb/s coherent system. *Opt. Express*, 16(2):873–879, Jan 2008.

[15] M.G. Taylor. Coherent detection method using dsp for demodulation of signal and subsequent equalization of propagation impairments. *IEEE Photonics Technology Letters*, 16(2):674–676, 2004.

[16] ZION. Understanding attenuation loss in optical fiber and how to minimize it. https://hello-signal.com/understanding-attenuation-loss-in-optical-fiber-and-how-to-minimize-it/.

[17] Govind Agrawal. *Fiber-Optic Communication Systems: Fourth Edition*. 2012.

[18] G.J. Foschini and C.D. Poole. Statistical theory of polarization dispersion in single mode fibers. *Journal of Lightwave Technology*, 9(11):1439–1456, 1991.

[19] Govind P Agrawal. Nonlinear fiber optics. *Nonlinear Science at the Dawn of the 21st Century*, 2000.

[20] Andrea D'Amico, Bruno Correia, Elliot London, Emanuele Virgillito, Giacomo Borraccini, Antonio Napoli, and Vittorio Curri. Scalable and disaggregated ggn approximation applied to a c+l+s optical network. *Journal of Lightwave Technology*, 40:1–1, 06 2022.

[21] L. Bayvel D. Guenther, D.G. Steel. *Encyclopedia of Modern Optics*. 2004.

[22] E. Desurvire. Analysis of noise figure spectral distribution in erbium doped fiber amplifiers pumped near 980 and 1480 nm. *Appl. Opt.*, 29(21):3118–3125, Jul 1990.

[23] Michael Connelly. *Semiconductor Optical Amplifiers*. 01 2004.

[24] Yasutake Ohishi Makoto Shimizu Shoichi Sudo Kazuo Fujiura, Terutoshi Kanamori and Makoto Yamada. *Optical Fiber Amplifiers: Materials Devices and Application Technologies*. Artech house, 1997.

[25] Clifford Headley and Govind P. Agrawal. Raman amplification in fiber optical communication systems. Academic Press, 2005.

[26] Vittorio Curri. Gnpy model for design of open and disaggregated optical networks. In *2021 European Conference on Optical Communication (ECOC)*, pages 1–86, 2021.

[27] Mattia Cantono, Dario Pilori, Alessio Ferrari, Clara Catanese, Jordane Thouras, Jean-Luc AugÃ©, and Vittorio Curri. On the interplay of nonlinear interference generation with stimulated raman scattering for qot estimation. *Journal of Lightwave Technology*, 36(15):3131–3141, 2018.

[28] Vittorio Curri. Software-defined wdm optical transport in disaggregated open optical networks. In *2020 22nd International Conference on Transparent Optical Networks (ICTON)*, pages 1–4, 2020.

[29] Alessio Ferrari, Mark Filer, Karthikeyan Balasubramanian, Yawei Yin, Esther Le Rouzic, Jan Kundrat, Gert Grammel, Gabriele Galimberti, and Vittorio Curri. Gnpy: an open source application for physical layer aware open optical networks. *Journal of Optical Communications and Networking*, 12(6):C31–C40, 2020.

[30] A.E. Ozdaglar and D.P. Bertsekas. Routing and wavelength assignment in optical networks. *IEEE/ACM Transactions on Networking*, 11(2):259–272, 2003.

[31] Ireneusz Szcześniak, Andrzej Jajszczyk, and Bożena Woźna-Szcześniak. Generic dijkstra for optical networks. *J. Opt. Commun. Netw.*, 11(11):568–577, Nov 2019.

[32] Akbar Ghaffarpour Rahbar. Review of dynamic impairment-aware routing and wavelength assignment techniques in all-optical wavelength-routed networks. *IEEE Communications Surveys Tutorials*, 14(4):1065–1089, 2012.

[33] telecominfraproject. Gnpy. https://github.com/Telecominfraproject/oopt-gnpy.

[34] Vittorio Curri. Gnpy model of the physical layer for open and disaggregated optical networking [invited]. *Journal of Optical Communications and Networking*, 14(6):C92–C104, 2022.

[35] telecominfraproject. Gnpy with an ols system, 2019.

[36] Bruno Correia, Rasoul Sadeghi, Emanuele Virgillito, Antonio Napoli, Nelson Costa, Joao Pedro, and Vittorio Curri. Networking performance of power optimized c+l+s multiband transmission. In *GLOBECOM 2020 - 2020 IEEE Global Communications Conference*, pages 1–6, 2020.

[37] telecominfraproject. Json input files.

[38] FiberLabs Inc. Optical communication band, March, 2023.

[39] Ieee standard for information technology– local and metropolitan area networks– specific requirements– part 3: Csma/cd access method and physical layer specifications amendment 4: Media access control parameters, physical layers, and management parameters for 40 gb/s and 100 gb/s operation. *IEEE Std 802.3ba-2010 (Amendment to IEEE Standard 802.3-2008)*, pages 1–457, 2010.

[40] Ieee standard for ethernet - amendment 10: Media access control parameters, physical layers, and management parameters for 200 gb/s and 400 gb/s operation. *IEEE Std 802.3bs-2017 (Amendment to IEEE 802.3-2015 as amended by IEEE's 802.3bw-2015, 802.3by-2016, 802.3bq-2016, 802.3bp-2016, 802.3br-2016, 802.3bn-2016, 802.3bz-2016, 802.3bu-2016, 802.3bv-2017, and IEEE 802.3-2015/Cor1-2017)*, pages 1–372, 2017.

[41] Open ROADM. Open roadm msa device white paper, April, 2024.

[42] Open ZR+. Open zr+ msa, September, 2023.

[43] International Telecommunication Union. Optical transport network security, December, 2021.

[44] ADVA security. Layer 1 encryption.

[45] Pan Dacom Direct. Basics layer 1, 2 and 3 encryption.

[46] Ribbon Communications. What is layer 1 encryption?